TRƯỜNG ĐẠI HỌC QUY NHƠN
QUY NHON UNIVERSITY

TẠP CHÍ KHOA HỌC
JOURNAL OF SCIENCE

CHUYÊN SAN KHOA HỌC TỰ NHIÊN VÀ KỸ THUẬT
ISSUE: NATURAL SCIENCES AND ENGINEERING

16 (3)
2022

BÌNH ĐỊNH, 6/2022

JOURNAL OF SCIENCE
QUY NHON UNIVERSITY
https://js.qnu.edu.vn
Vol. 16, N° 3, 2022
ISSN : 1859-0357

CONTENTS

TẠP CHÍ KHOA HỌC
TRƯỜNG ĐẠI HỌC QUY NHƠN

Formamide - một tiền chất sinh học của DNA nucleobase: Đường phản ứng tạo thành theo gốc tự do

Huyền Thị Nguyễn[1], Yassin A. Jeilani[2] and Minh Thọ Nguyễn[1,*]

[1]Khoa Hóa học, Trường Đại học Leuven, Vương quốc Bỉ
[2]Khoa Hóa học, Trường Đại học Hail, Ả Rập Saudi
[2]Khoa Hóa học và Sinh Hóa, Đại học Spelman, Atlanta, Mỹ

Ngày nhận bài: 13/12/2021; Ngày nhận đăng: 28/4/2022

TÓM TẮT

Trong bài tổng quan này, chúng tôi tóm lược các cơ chế phản ứng tạo thành các chất nucleobase của DNA từ formamide (FM) theo các con đường phản ứng gốc tự do đã được nghiên cứu bằng các tính toán hóa học lượng tử. Formamide được biết đến như một tiền chất của nucleobase có từ thời Trái đất sơ khai, hoặc trong bầu khí quyển ngoài trái đất giàu nitơ như hành tinh Titan, trong điều kiện có nước cũng như không có nước. Hiện nay các thí nghiệm mô phỏng trong phòng thí nghiệm về các điều kiện ngoài Trái đất gặp nhiều khó khăn vì kiến thức còn rất hạn chế về các môi trường chưa được khảo sát thực tế, do khoảng cách quá xa. Tuy nhiên, các bằng chứng quang phổ ngày càng chứng minh cho giả thiết là các hợp chất hữu cơ đã được tìm thấy trong bầu khí quyển Titan. Sự hình thành các phân tử phức tạp trong những môi trường như vậy có thể được hình thành thông qua các con đường phản ứng gốc tự do. Các gốc hóa học tự do tạo nên nhiều con đường phong phú, độc đáo cho quá trình hình thành các phân tử sinh học từ những hợp chất hữu cơ đơn giản. Chúng thúc đẩy hơn nữa sự hiểu biết của chúng ta trong quá trình tổng hợp các hợp chất tiền sinh học từ các hợp chất hữu cơ dị vòng. Tất cả các cơ chế được đề xuất sử dụng các phản ứng gốc đơn giản như sự dịch chuyển các nguyên tử H, sự tấn công của các gốc tự do nhỏ như $^{\bullet}H/^{\bullet}OH/^{\bullet}NH_2$… Ưu điểm của cơ chế phản ứng gốc tự do là hầu hết các phản ứng quan trọng đều có hàng rào năng lượng tương đối thấp. Những đường phản ứng khác nhau này dẫn đến sự hình thành một hỗn hợp sản phẩm, dẫn đến sự đa dạng trong các phân tử sinh học được hình thành từ một số nhỏ hợp chất ban đầu đơn giản.

Từ khoá: *Formamide, tiền chất sinh học, sự hình thành của DNA nucleobase, phản ứng hóa học gốc tự do*.

Corresponding author.
Email: minh.nguyen@kuleuven.be

JOURNAL OF SCIENCE
QUY NHON UNIVERSITY

Formamide as a prebiotic precursor of DNA nucleobases: The free radical routes

Huyen Thi Nguyen[1], Yassin A. Jeilani[2] and Minh Tho Nguyen[1,*]

[1]Department of Chemistry, KU Leuven, Belgium
[2]Department of Chemistry, University of Hail, Saudi Arabia
[2]Department of Chemistry and Biochemistry, Spelman College, Atlanta, USA

Received: 13/12/2021; Accepted: 28/4/2022

ABSTRACT

In this review we probe the reaction mechanisms for formation of DNA nucleobases from formamide (FM) following the free radical pathways that have been identified by quantum chemical computations. Formamide is known as a precursor of nucleobases in the prebiotic chemistry of the Early Earth or in the nitrogen-rich atmosphere such as Titan, regardless of whether water is present or absent. Laboratory simulation experiments of the extra-terrestrial conditions are not trivial to setup because of the limited knowledge of the unseen environments. However, increasing synthetic and spectral evidence for organic compounds have been found in the organic haze of Titan's atmosphere. Formation of complex molecules under such environments can be expected to proceed in part through free radical pathways. The free radicals constitute promising routes for the nonthermal construction of biomolecules. They further promote our understanding in the prebiotic synthesis of heterocyclic organic compounds. All of the suggested mechanisms employ simple radical reactions such as H rearrangements (shifts), ●H/●OH/●NH_2 radical losses, and most importantly intramolecular radical 1, n-cyclization. The advantages of free radical mechanisms are the inherently low energy barriers that are observed in most reaction steps and the highly exergonic nature of the whole reaction chains. The channels lead to more than one product at the end, which brings in the concept of diversity in biomolecules formed from a single prebiotic route.

Keywords: *Formamide, prebiotic chemistry, formamide in prebiotic chemistry, DNA nucleobases formation, free radical routes.*

1. THE ORIGIN OF LIFE: A BOTTOM-UP APPROACH

Sometimes just a single discovery is needed to break down the limiting walls of knowledge. A discovery that broke down the wall between organic and inorganic chemistry was the synthesis of a simple organic molecule (urea $(NH_2)_2CO$) from two inorganic compounds (AgNCO + NH_4Cl) by Friedrich Wöhler in 1828.[1] A breakthrough in prebiotic chemistry started more than one century later in 1953 with the Miller-Urey experiment showing the possibility of spontaneous beginning of life in the Early Earth.[2,3] The Miller's group was the first to design experiments in the perspective of the 'Darwin's prebiotic soup'. A mixture of CH_4, NH_3, H_2 and H_2O vapor was put in the reactor to mimic the supposed components of the primitive reducing Earth atmosphere closed to a sample of 'early ocean', along with electrodes used for electric discharges to simulate lightning. After seven days, Stanley Miller and Harold Urey

**Corresponding author.*
Email: minh.nguyen@kuleuven.be

https://doi.org/10.52111/qnjs.2022.16301

found several amino acids in the ocean flask in this closed medium, and the product mixture includes alanine, glycine, aspartic acid and α-amino butyric acid. This experiment really initiated the subject of origin of life as a scientific research topic. Inspired by this discovery, many subsequent simulation experiments were carried out confirming the possibility of formation of different building blocks of biomolecules from simple prebiotic molecules. Subsequent studies suggested that the early atmosphere might contain less CH_4 and more CO_2, and the localized environments could have near volcanic activities. The abiotic syntheses were subsequently reported for nucleobases,[4-8] sugars,[9] nucleotides,[10] and amino acids.[4,11] Formation of amino acids was shown to be more difficult in experiments using CO_2 instead of CH_4. Variations of Miller's experiments carried out include aspects of hydrothermal vents, neutral atmospheres, reducing H_2S atmospheres, volcanic conditions, etc. In each of these variations amino acids or organic precursors of amino acids could be identified.

Formation of these building blocks from simpler inorganic starting materials[12] was considered as the first step in the bottom-up approach which explores the chemical processes in going from the simpler to the more complex systems (Scheme 1.1).[12] The bottom-up approach starts with some simple prebiotic molecules and conditions that mimic the chemical conditions on the Early Earth, and attempts to understand the formation of building blocks and biomolecules, the catalysis and the self-organizations.

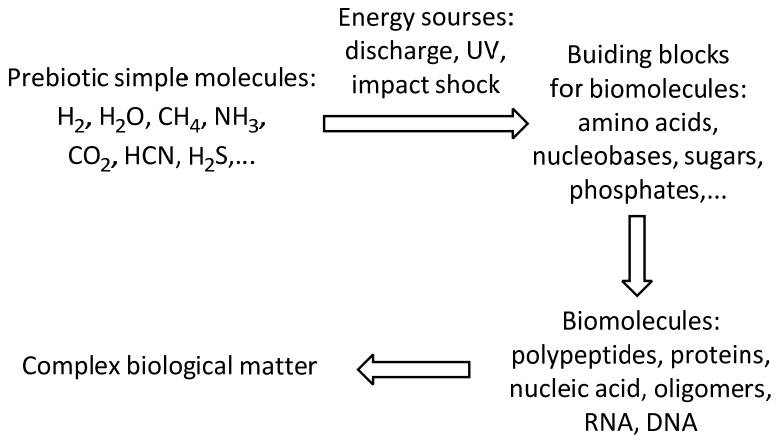

Scheme 1. Sequential steps of the bottom-up approach for the origin of life.[12]

Organic compounds leading to the birth of terrestrial organisms can be abiotically synthesized in the primitive atmosphere and/or ocean of the Earth. The primeval atmosphere of the Earth which is usually hypothesized to be composed of simple molecules, can be those detected in interstellar space, or having similar composition to some bodies of the Solar system such as Mars, Titan or Europa.[2,13,14] These early building blocks of life could also be formed extra-terrestrially and brought to our planet by meteorites or comets. Many molecules including important prebiotic precursors such as HCN, HNCO, H_2CO, NH_2CHO, HCOOH, etc., and larger cyclic and acyclic organic compounds have been detected in the interstellar medium mostly by means of molecular spectroscopy (see Table 1 for the census in 2013).[15-17] The affluence of extra-terrestrial molecules clearly suggests the existence of active chemical processes taking place in the interstellar medium, which eventually may result in the syntheses of precursors and building blocks for biomolecules. Several amino acids including glycine, alanine, glutamic acid, valine, and proline, and nucleobases including xanthine and uracil, are present in the interstellar medium, comets, and meteorites.[18-20] The non-terrestrial origin of xanthine and uracil has been confirmed using compound-specific carbon isotope data of the Murchison meterorite.[20]

Table 1. Temporary census of interstellar molecules.[17]

Types	List of molecules
2 atoms	AlCl, AlF, AlO, C_2, CF^+, CH, CH^+, CN, CN^-, CO, CO^+, CP, CS, FeO, H_2, HCl, HCl^+, HF, NH, KCl, N_2, NO, NS, NaCl, O_2, OH, OH^+, PN, SH, SH^+, SO, SO^+, SiC, SiN, SiO, SiS, PO
3 atoms	AlNC, AlOH, C_3, C_2H, C_2O, C_2P, C_2S, CO_2, H_3^+, CH_2, H_2Cl^+, H_2O, H_2O^+, HO_2, H_2S, HCN, HCO, HCO^+, HCS^+, HCP, HNC, HN_2^+, HNO, HOC^+, KCN, MgCN, NH_2, N_2H^+, N_2O, NaCN, OCS, SO_2, c-SiC_2, SiCN, SiNC, FeCN
4 atoms	C_2H_2, l-C_3H, c-C_3H, C_3N, C_3O, C_3S, H_3O^+, H_2O_2, H_2CN, H_2CO, H_2CS, HCCN, $HCNH^+$, HCNO, HOCN, $HOCO^+$, HNCO, HNCS, HSCN, NH_3, SiC_3, PH_3
5 atoms	C_5, CH_4, c-C_3H_2, l-C_3H_2, H_2CCN, H_2C_2O, H_2CNH, H_2COH^+, C_4H, C_4H^-, HC_3N, HCCNC, HCOOH, NH_2CN, SiC_4, SiH_4, HCOCN, HC_3N^-, HNCNH, CH_3O
6 atoms	c-H_2C_3O, C_2H_4 , CH_3CN, CH_3NC, CH_3OH, CH_3SH, l-H_2C_4, HC_3NH^+, NH_2CHO, C_5H, HC_2CHO, HC_4N, CH_2CNH, C5N^-, HNCHCN
7 atoms	c-C_2H_4O, CH_3C_2H, H_3CNH_2, CH_2CHCN, H_2CHCOH, C_6H, C_6H^-, HC_4CN, CH_3CHO, HC_5N^-
8 atoms	H_3CC_2CN, $H_2COHCOH$, CH_3OOCH, CH_3COOH, C_6H_2, CH_2CHCHO, CH_2CCHCN, C_7H, NH_2CH_2CN, CH_3CHNH
9 atoms	CH_3C_4H, CH_3OCH_3, CH_3CH_2CN, CH_3CONH_2, CH_3CH_2OH, C_8H, HC_6CN, C_8H^-, CH_2CHCH_3
> 9 atoms	CH_3COCH_3, CH_3CH_2CHO, CH_3C_5N, HC_8CN, CH_3C_6H, $CH_3OC_2H_5$, $HC_{10}CN$, C_6H_6, C_2H_5OCHO, C_3H_7CN, C_{60}, C_{70}, C_{60}^+
Deuterated	HD, H_2D^+, HDO, D_2O, DCN, DCO, DNC, N_2D^+, NHD_2, ND_3, HDCO, D_2CO, CH_2DCCH, CH_3CCD, D_2CS

In addition to the open questions about the starting materials needed for the prebiotic synthesis in the Early Earth, the conditions under which the earliest form of life was triggered remain unidentified. Various simulation experiments have been carried out under different hypothetically prebiotic conditions. The well-known Miller-Urey experiment is a typical example of the gas phase reactions driven by electric discharges, which might have occurred in the primitive Earth atmosphere.[2,3] Simple heating of prebiotic molecules[21] or their solutions[7] mimics the possible prebiotic chemistry that took place during meteorite/comet impacts, volcanic activities or near the hydrothermal vents on the ocean floor. These experiments were carried out to seek for the high-temperature origin of life, which has been suggested on the basis of the fact that hyperthermophiles ('superheat-loving' micro-organisms) were claimed to "occupy all the short deep branches closest to the root" of the phylogenetic tree of life.[22] However, some authors contradicted this idea giving the reason that "even if they are the oldest extant organisms, which is in dispute, their existence can say nothing about the temperatures of the origin of life", and "there is no geological evidence for the physical setting of the origin of life".[23]

Furthermore, the fast degradation of the biomolecular building blocks at high temperature also casts doubt on the possibility of life emergence in hot condition.[24] The low-temperature origin of life thus concurrently emerged with numerous simulation experiments demonstrating its feasibility. Some examples of the cold prebiotic synthesis include the

https://doi.org/10.52111/qnjs.2022.16301

formation of adenine from the frozen solution of HCN and NH_4OH,[25] and the synthesis of cytosine and uracil from eutectic solution of cyanoacetaldehyde with guanidine or urea.[26] These prebiotic reactions could take place in the frozen regions of the primitive Earth, in some planets and satellites with water-ice crust such as Europa, the moon of Jupiter, or in the ice mantles on the surface of interstellar grains.[27,28]

The efficiency of the biomolecule synthesis partly depends on the concentration of starting materials in the primeval soup. This problem has been solved in both high - and low-temperature origin-of-life theories. The high temperature induces the evaporation of accent water reservoirs resulting in an increase of concentrations of precursor molecules (drying-lagoon or drying-beach model).[29] It is obvious that this model cannot apply to volatile molecules or azeotropic mixtures. In these situations, the solute molecules could be concentrated upon eutectic freezing in which the solute molecules are excluded from the ice matrix and trapped inside the "interstitial brines" with much higher concentrations.[26] Minerals can also play an important role in the prebiotic chemistry due to their ability to accumulate the precursor molecules on their surfaces.[30,31] They can also provide restrictions in molecular orientations, catalyze surface reactions, stabilize high-energy intermediates and protect newly-formed products with high degradation rates.[32-35]

Life, as we know it today, consists of two interacting processes called metabolism and replication with possible representatives being proteins and RNA/DNA molecules, respectively. Most origin-of-life theories within the bottom-up approach belong to two opposite categories depending on which type of molecules was formed first (from the mixture of biomolecular building blocks formed in the prebiotic soup). The 'metabolism-first' hypothesis suggests that the early life is characterized by a series of self-sustaining chemical networks, and information replication would appear when the complexity of these networks of reactions evolves over time. The 'replication-first' hypothesis, on the contrary, suggests that molecules with the ability to store and transmit genetic information to descendants were the first molecules of life. Typical examples of metabolism- and replication-first theories are 'Iron-Sulfur World' and 'RNA World' scenarios, respectively. The Iron-Sulfur World (ISW) scenario, first proposed by Wächtershäuser in 1988,[36,37] presents a premise that a series of reactions representing simple catabolism cycles could occur under catalytic effects of iron sulphide minerals near hydrothermal vents. For example, the pyrite FeS_2 mineral can be reduced by H_2S gas emitted from hot vents to FeS, which in turn reduces CO or CO_2 to form more complex organic molecules such as acetic acid, pyruvic acid ($CH_3COCOOH$) and alanine ($CH_3CH(NH_2)COOH$), and subsequently changes back to FeS_2.[38] On the other hand, the RNA World hypothesis suggests that RNA is the original life molecule with both catalytic and replication functions.[39] The nucleobases and sugars, which are readily formed from simple prebiotic molecules as mentioned above, could combine to form nucleotides and subsequently RNA, possibly under catalytic effects of minerals. While a solid answer for this 'chicken and egg' question has not been found yet, a common chemical frame which can generate building block molecules of both metabolism and replication processes — both amino acids and nucleobases, for example — would be a favourable choice for investigation.

2. FORMAMIDE AS A PREBIOTIC PRECURSOR

Formamide (NH_2CHO, FM), the simplest member of the amide functional group, recently attracted great interest in the field of prebiotic syntheses for several reasons.

A recent report[40] on FM and the origin of life stated that: 'The most abundant three-atoms organic compound in interstellar environment is hydrogen cyanide HCN, the most abundant three-atoms inorganic compound is water H_2O. The combination of the two results in the formation of formamide.' HCN is a key precursor

https://doi.org/10.52111/qnjs.2022.16301

for prebiotic synthesis because its well-known polymerization reactions in the presence of water yield a variety of important biomolecules under various conditions.[4-8,11,41]

In 1961, Oró reported the synthesis of adenine from hydrogen cyanide (HCN) in aqueous ammonia at moderate temperature (27−100 °C).[7] Hydrolysis of concentrated ammonium cyanide (NH_4CN) solution yielded a variety of nucleobases[4-6,8] such as adenine, guanine, uracil, and hypoxanthine, and other pyrimidine derivatives[41] such as orotic acid, 5-hydroxyuracil, and 4,5-dihydroxylpyrimidine. Urea and several amino acids including glycine, alanine, aspartic acid and serine were also detected as hydrolysis products of HCN.[11] The role of HCN as 'absolute protagonist' was therefore suggested.[42]

However, high concentration of HCN, required for an efficient polymerization, is in fact quite difficult to achieve in the conditions of the Early Earth, especially in the hot condition because HCN is more volatile than water.[43] Hydrolysis of HCN producing FM was reported to become dominant when the concentration of HCN is reduced to < 0.01 M.[44]

Similar to HCN, FM is also a potentially prebiotic molecule. It has widely been detected in the interstellar medium,[15-17] comets such as C/1995 O1 (Hale-Bopp),[45] C/2012 F6 (Lemmon) and C/2013 R1 (Lovejoy),[46] and also in the inner cores of two high-mass star-forming regions, NGC 6334(I) and G327.3-0.6.[47] With limited azeotropic effect, FM can easily be concentrated upon heating its dilute solution. Furthermore, it remains in the liquid state within a wide temperature range of 4–210 °C,[42] and could thus serve as a solvent for other prebiotic molecules.

Higher molecular complexity is a particular advantage of FM over HCN as a prebiotic precursor. FM contains four important elements of organic compounds, namely, C, H, O, and N, which allows formation of building blocks for biomolecules, even in the non-aqueous conditions. FM fragmentations form a wide range of low molecular weight products that can take part in further synthesized reactions including HCN, HNC, HNCO, HOCN, NH_3, H_2O, etc.[48-53]

Early in the 1970's, Boden and Back carried out various experiments to study the photolysis of FM under 206.2 nm radiation within the temperature and pressure ranges of 115−400 °C and 8−50 torr, respectively.[48] CO, H_2, and NH_3 were detected as reaction products with the highest yield being the production of CO. The authors proposed five reaction channels (1) – (5) upon photoexcitation of FM including C−N, C−H, and N−H bond dissociations, decarbonylation and dehydrogenation. The decarbonylation (4) is also the main thermal decomposition channel of FM at much higher temperature range of 1690 and 2180 K.[49]

$$NH_2CHO + h\upsilon \rightarrow NH_2 + H + CO \quad (1)$$
$$\rightarrow NH_2CO + H \quad (2)$$
$$\rightarrow NHCHO + H \quad (3)$$
$$\rightarrow NH_3 + CO \quad (4)$$
$$\rightarrow H_2 + HNCO \quad (5)$$

Photodecomposition of FM in low-temperature matrices revealed two main channels.[50] In Ar matrices, irradiation of FM excites the molecule to its first excited singlet S_1 state where the C–N bond cleavage forms a radical pair HCO + NH_2. The subsequent rapid dissociation of the HCO radical releases H•, which immediately combines with the NH_2 radical to form NH_3. However, in Xe matrices, the effect of the external heavy atom induces an intersystem crossing from the S_1 to the first triplet T_1 state energy surface, leading to a dehydrogenation giving HNCO + H_2 as main

https://doi.org/10.52111/qnjs.2022.16301

products, instead of NH_3 + CO. The C−N, C−H, and N−H homolytic bond dissociations were also suggested to take place on the T_1 energy surface in a photolysis study of FM at 205 nm.[51] Isocyanic acid (HNCO), which is the simplest [CHON] species, is a typical product in prebiotic simulation experiments,[54,55] and can take part in future synthesis such as urea formation.[56]

In addition, the dehydration channel generating back the triatomic products HCN/HNC from FM has also been reported.[48,52,53] Thermal decomposition of FM at 185 °C produces three gaseous products CO_2, CO, and NH_3 along with a black insoluble polymer of HCN whose pyrolysis gives raise to HCN, NH_3 and HNCO.[52] Upon heating FM to 220 °C, HCN is also detected in the gaseous products. A trace amount of HCN was also detected when an unfiltered mercury arc is used as a light source for FM photolysis.[48] When heating FM on the TiO_2 surface, the dehydration of FM yielding HCN becomes one of the two main decomposition pathways (the other pathway being decarbonylation).[53]

Other organic compounds with important prebiotic role can also be synthesized from FM in the presence of catalysts.[40,57,58] For example, formaldehyde (HCHO), a precursor of sugars,[59-61] and formic acid (HCOOH), a precursor of lipids,[62] were detected in the product mixture when heating FM with TiO_2.[57] The latter was also observed as main decomposition product of FM in pressurized hot water at the temperatures of 573–693 K and pressure of 23 MPa.[58]

Despite the fact that all the decomposition products of FM were already detected in space, their presence as both reactants and catalysts in the reaction mixture starting from only one starting material, FM, is remarkable because they can facilitate many other product channels. Syntheses of various biologically relevant compounds such as nucleobases, amino acids, carboxylic acids, and other important prebiotic intermediates from FM have extensively been reported in the literature (cf. Table 2).[21,57,63-78]

Table 2. List of biologically relevant compounds synthesized from FM that have been reported in the literature.[21,57,63-78]

Types	Names
Primary RNA/DNA nucleobases	adenine, guanine, cytosine, uracil, and thymine
Purine derivatives	purine, 2-aminopurine, N^9-formylpurine, 9-(hydroxyacetyl)purine, 9-[2,3-dihydroxy-1-(oxo)propyl]purine, N^6,N^9-diformyladenine, N^6-formyl-9-(hydroxyacetyl)adenine, hypoxanthine...
Pyrimidine derivatives	5-hydroxy-pyrimidine, 2(1H)-pyrimidinone, 4(3H)-pyrimidinone, isocytosine, and 5,6-dihydrouracil...
Five-membered rings	5-aminoimidazole-4-carboxamide (AICA), 5-formamidoimidazol-4-carboxamide (fAICA), hydantoin, and glycocyanidine...
Amino acids and related compounds	2-aminobutanoic acid, 2-methylalanine, β-alanine, β-amino isobutyric acid (β-AIBA), alanine, aspartic acid, glycine, glyoxylamine, hydroxyproline, leucine, N-formylalanine, N-formylglycine, N-methylglycine, phenylalanine, valine, and tert-leucine...
Carboxylic acids	2,3-dihydroxypropanoic, 2,4-dihydroxybutanoic, 3,4-dihydroxybutanoic, α-ketoglutaric, acetic, ethanimidic, fumaric, glycolic, glyoxylic, hexanoic, lactic, maleic, malic, malonic, nonanoic, octanoic, oxalic, oxaloacetic, parabanic, pimelic, propanoic, pyruvic, and succinic acids...
Others	urea, guanidine, guanidine acetic acid, dihydroxy acetone, diaminomalonitrile (DAMN), carbodiimine, and isocyanate...

The addition of a catalyst is necessary for the synthesis of nucleobases when heating neat FM in the temperature range of 130 − 200 °C without irradiation because otherwise only purine is formed.[63] Various substances have been used to catalyze these reactions including calcium carbonate,[21,68] phosphates,[66,68] borate minerals,[74] zeolite, alumina and silica,[21] clays,[21,64,77] titanium dioxide,[57,72,77] iron sulfur and iron-copper sulfur,[67] iron oxide and iron oxide hydroxides,[73] zirconium minerals,[70] metal octacyanomolybdates,[76] cosmic dust analogues,[65] and meteorites.[71,75,77] In the presence of Campo del Cielo meteorite, a large number of organic compounds were synthesized from FM even in dilute solution (FM/water = 1/10 v/v).[75]

On the other hand, irradiation with soft UV light (320 nm) during the heating process was proven to facilitate the production of nucleobases even without adding a catalyst.[77] Nucleobases can also be formed from FM under high-energy meteoritic impact conditions. Irradiation of ice or liquid FM with high-power laser beam yielded purine, glycine and all five primary nucleobases.[77] The extremely high temperature of 4500 K in the laser spark creates hot dense plasma containing highly reactive radicals such as $^{\bullet}NH_2$, $^{\bullet}NH$, and $^{\bullet}CN$, which were suggested to be involved in the formation of nucleobases. Free radicals were also previously reported in the reaction mixture of the Miller-Urey's experiment.[2] Free radical mechanisms were therefore suggested for the formation of nucleobases from FM, which constitute the main subject of the present review.

Obviously, despite the highly diverse transformation network from FM, many links are still missing on the path leading from FM to the formation of the first molecules of life. One step further toward formation of information molecules from FM was the formation of acyclo-nucleosides when heating neat FM in the present of TiO_2 under sunlight irradiation.[57] These acyclo-nucleosides were suggested to react with phosphate-rich surfaces (possible source of phosphate in nucleotides), followed by 'formamide-mediated transphosphorylation.'[42] Such a scheme indeed sounds hypothetical, considering the concentration of FM needed for the formation of acyclo-nucleosides and their polymerization. However, this scheme proposed possible solutions for the formation of nucleotides and the stability of the oligomers/polymers formed from these nucleotides.[42]

As long as the answer for the question of life's origin has not been found yet, intriguing hypotheses that could explain the development from prebiotic to biotic periods in the history of life on Earth will continuously be proposed. Both experimental and theoretical researches in the prebiotic chemistry, that were/are based on the results of an evaluation of the hypotheses, and then propose some new ones, would ultimately bring us closer and closer to the true answer.

Let us mention that Titan is the largest moon of Saturn with a thick atmosphere containing a considerable amount of complex organic compounds. Formation and fate of these organics within the atmosphere or on the surface of Titan follow quite complex processes. Photochemical reactions[79] and gas phase reactions induced by high-energy solar radiation in Titan's atmosphere[80] were postulated to lead to formation of organic compounds, including nucleobases. There is in fact growing evidence that nucleobases can be formed on Titan's surface.[81-84] Formation of adenine was reported when Titan aerosol analogues were exposed to soft X-ray irradiation and secondary electrons.[81] Nucleobases including adenine and guanine may be formed in Titan's atmosphere.[84] These simulation experiments used a coupled radio frequency discharge to initiate the reactions of a mixture of gases (CH_4, N_2, and CO).

Both aqueous and non-aqueous syntheses of the nucleobases were considered. The non-aqueous scenario was preferred because the nucleotides formed in subsequent steps are not stable in aqueous media.[85] Because of such an instability, a recent study considered mechanisms for the non-aqueous scenario formation of nucleobases from FM on Earth.[86]

https://doi.org/10.52111/qnjs.2022.16301

Even more important is the fact that this scenario is consistent with the formation of nucleobases in a non-aqueous extra-terrestrial environment.

Theoretical studies pointed out that formation of nucleobases is associated, with high energy barriers.[87] To lower the energy barriers water has been included along the pathways.[88] For example, a study using density functional theory (DFT) showed a potential water-catalyzed pathway for adenine formation starting from FM.[89-91] Involvement of water in the reactions was in deed necessary in lowering the energy barriers.[92] These studies suggested some compelling mechanisms for the formation of one nucleobases. However, they cannot be used to explain the formation of nucleobases from a non-aqueous scenario because there is no water as required to lower the energy barriers.

The presence of minerals such as pyrite, kaolinite etc. could also catalyse prebiotic reactions of formamide.[93,94] Under radiation, the reactions could be achieved in excited states.[95]

3. THE FREE RADICAL ROUTES

The prebiotic Earth environment might have restricted the types of possible reactions that could have been prevalent on Earth. Most probably, the lack of an ozone layer, an oxygen depleted atmosphere, and the high flux of solar UV irradiation had impact on the transformations. Such conditions promoted electron-transfer processes inducing free-radical routes. Recent studies indicated involvement of free radicals in the prebiotic pathways.[83,96] For example, laboratory experiments to simulate high-energy impact events on Earth with an extra-terrestrial icy body showed products that were formed from the reaction of free radicals with FM.[96] Also, formation of organic molecules on Titan's atmosphere was suggested featuring free-radical pathways.[97-99]

FM reactions are related to the prebiotic HCN reactions because FM can be considered as the hydrolysis product of HCN. The latter has in fact been detected on Titan.[79] Ultraviolet (UV) photolysis or proton irradiation of HCN, NH_3 and water ice gave FM as a product.[100] In principle, FM as well as HCN, in either the neutral or the radical form, could both be carbon-containing building blocks for prebiotic synthesis in interstellar medium or on Titan's surface.

In the search for the origin of nucleobases, reaction of the ●CN radical with FM has recently been studied to identify nucleobase-intermediates and to better understand the reactivity of FM.[96] Controlled reactions of FM with ●CN led to the identification of 2-amino-2-hydroxyl-acetonitrile as a possible precursor for nucleobases.[96] Moreover, the role of ●CN toward nucleobase synthesis has also been considered through the formation of the important intermediates, diaminomaleonitrile (DAMN) and diaminofumaronitrile (DAFN).[97] Previous theoretical studies of mechanisms for the production of nucleobases from FM reactions yielded pathways with relatively high energy barriers.[89-91,101] In the last decade, there have been a large amount of studies, both experimental and theoretical alike, devoted to the formation of nucleobases from formamide. Perhaps most aspects of these prebiotic processes have been explored in much detail.[102-128,135-146]

In view of the important role of formamide (FM) in prebiotic chemistry, we would focus in this review on the free radical routes leading to generation of purine and pyrimidine nucleobases from FM, that are also appropriate for a prebiotic synthesis of nucleobases on Titan. Because the one-pot synthesis from FM can give both purines and pyrimidines, it is reasonable to expect that there exists a set of free radical routes that leads to both purines and pyrimidines.[21,57,64-76]

Scheme 2 points out different reaction pathways including formation of purine and purine bases (adenine, guanine, hypoxanthine, xanthine, and isoguanine) and pyrimidine bases (cytosine, uracil, and thymine) starting from FM (1) and the small species which are present in the prebiotic atmospheres (in particular of Titan) such as HCN, ●CN, and $●NH_2$.

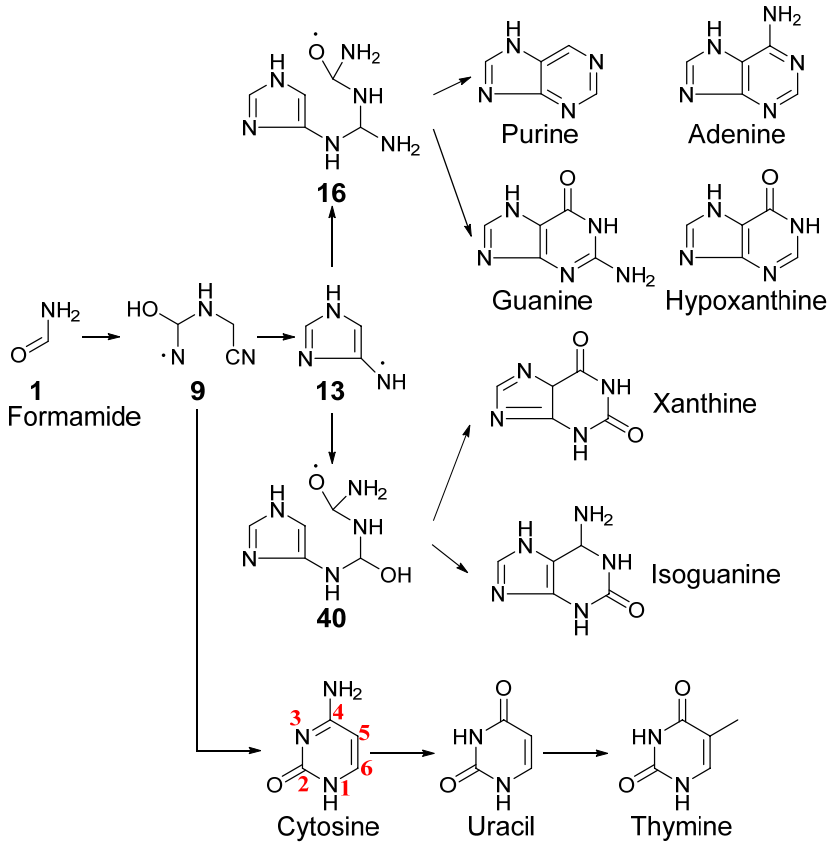

Scheme 2. Free radical pathways leading to the formation of purine and pyrimidine nucleobases from FM.

Relatively high yields of both purine and adenine were reported when FM was irradiated with UV light while heating.[68] Under prebiotic conditions, nucleobases can be produced following heating of FM but the yields of nucleobases are different from UV irradiation/heating conditions. These reactions likely involved free radicals that were produced via a thermally activated precursor or via photoexcitation of reaction intermediates.[95]

It should be noted that these suggested routes are only a small part of a far more complicated network of possible reaction pathways leading to nucleobases, and side radical reactions yielding other by-products could take place from the reactant mixture. There are major similarities in the types of reactions leading to both pyrimidine and purine bases. For example, some steps involved in the formation of both pyrimidine bases and purines include the hydrogen abstractions, hydrogen rearrangements, and cyclization steps. Also, these types of reactions can take place with intermediates and may lead to byproducts. These side reactions tend to decrease the yield. Indeed, these products were experimentally identified with low yields.[57,73] Further comprehensive studies of all the possible reactions, in both thermodynamic and kinetic aspects, are needed to give a firm conclusion on whether the formation of nucleobases is more competitive than other side reactions. In this context, we limited ourselves to consider in the present study several possible mechanistic routes that can ultimately lead to nucleobases. The main aim is to prove the probability of free radical mechanisms for their formation. At low temperature condition in Titan (less than 100 K), the potential energy profiles match very well with the enthalpy and Gibbs free energy profiles. The differences become larger when the temperature increases. Therefore, the effect of temperature on these suggested mechanisms is also examined to

validate their applicability for high temperature conditions (94 – 483 K).

Let us briefly mention that the energy profiles associated with the free radical mechanisms are constructed using density functional methods (DFT) Geometries of all the species involved are optimized using the hybrid B3LYP functional[129,130] with the 6-311G(d,p) basis set.[131] The unrestricted formalism (UB3LYP) is used for the open-shell structures. Vibrational frequency analyses are carried out at the same level of theory to obtain the zero-point correction energy (ZPE) and to confirm the nature of each stationary point. The minima have no imaginary frequencies while the first-order saddle points have one imaginary frequency. A uniform scaling factor of 0.967 is used for the ZPE values when calculating the relative energies of the structures considered. In fact, the scaling factor has a very small effect on the relative energies of different species on the potential energy profiles of FM reactions. The difference between the data calculated with and without scaling factor are less than 0.5 kcal/mol, which is negligible. Therefore, the scaling factor was not employed when calculating the enthalpy and Gibbs free energy data that includes the entropic changes.

The popular B3LYP functional has been employed in several previous studies to explore the production of nucleobases.[132] These studies showed that the difference between B3LYP and more accurate wavefunction methods such as the coupled-cluster theory CCSD(T) reaction barriers are relatively small, being less than ± 3 kcal/mol. In addition, DFT energy barriers for hydrogen-abstraction reactions have been previously reported to be in good agreement with experimental results.[133,134] Previous studies further suggest that the B3LYP functional can be appropriate for the free radical reaction calculations.[133,134]

The performance of the B3LYP/6-311G(d,p) method for radical pathway is validated in the present work for a short reaction chain starting from FM **1** to the radical species **6** as plotted in Scheme 3. As a convention, the minima involving in the radical reaction pathways are named as **1**, **2**, **3**, etc., and the transition structure (TS) connecting two minima, for example **1** and **2**, is denoted as **ts-1,2**. The CCSD(T) single point calculations are carried out using the B3LYP/6-311G(d,p) optimized geometries of the relevant species. Two basis sets used for the CCSD(T) calculations include 6-311G(d,p) and aug-cc-pVTZ. When using a large basis set for CCSD(T) computations the differences between two sets of data become smaller with the largest difference being ± 3 kcal/mol.

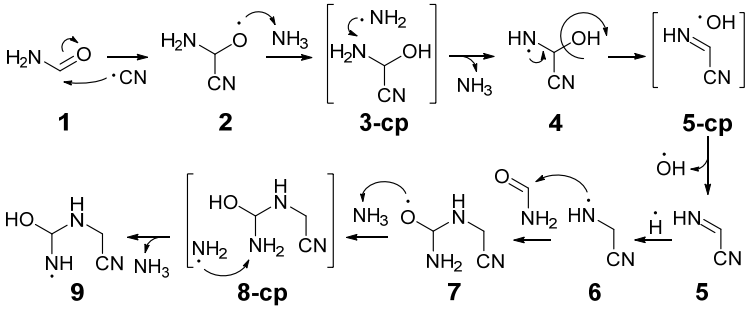

Scheme 3. Formation of the precursor **9**

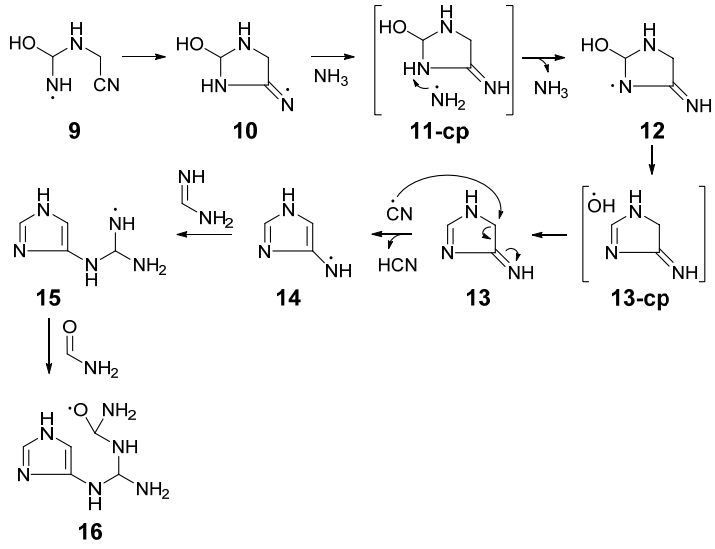

Scheme 4. Formation of the precursor **16**

3.1. Formation of the precursors 13 and 16

The suggested reaction mechanisms leading to the formation of purine nucleobases can be viewed as several reaction chains connected to each other by common precursors including **9**, **13**, **16** and **40** (cf. Scheme 2). In this section, we consider the formation of the two precursors **13** and **16** from FM. The current mechanisms predict an imidazole derivative **13** as a precursor for purine nucleobases, which is consistent with previous experimental observations.[96] Imidazole derivatives were readily converted to purines, including adenine, hypoxanthine, and guanine.[135] From this imidazol derivative, the precursor molecule **16** is formed leading to the synthesis of purine, adenine, guanine, and hypoxanthine, and the precursor molecule **40** leading to xanthine and isoguanine (cf. Scheme 2).

The free radical pathway for the formation of the imidazole precursor **13** starting from FM is presented in Schemes 3 and 4. The first step of the mechanism is an exergonic addition reaction of ●CN to FM **1** to give **2** (cf. Figure 1). In fact, this step is based on the reaction of ●CN with FM in an experimental work carried out by Ferus *et al*.[96] Coupling of a H radical with the oxygen-centered radical **2** leads to 2-amino-2-hydroxyacetonitrile,[3] an experimentally detected precursor for the nucleobases.[96]

To form 2-imino-acetonitrile **5** via a OH radical elimination step (**4** → **5-cp**), a H atom of the NH_2 group of oxygen-centered radical **2** needs to be transferred to the adjacent O atom to form nitrogen-centered radical **4**. This can be done via either a one-step or a multistep H-rearrangement reaction. The relatively high energy barrier for the 1,3-H radical transfer amounts to 25 kcal/mol. A similar 1,3-H radical rearrangement was previously described for guanine radicals in which the proposed reaction takes place through a five-membered ring with the assistance of water.[136]

The addition and abstraction of H radical are assisted by the neutral/radical pair NH_3/●NH_2 in a multistep reaction to reduce the energy barrier. Ammonia (NH_3) is selected for assisting the rearrangement because NH_3 has been reported as a constituent of the interior of Titan that feeds its atmosphere by episodic effusive events.[137] Moreover, NH_3 has been suggested to play an important role in prebiotic reactions, as it is a decomposition product of FM, without or with the presence of water.[136,138-139]

The multistep reaction transforming **2** to **4** consists of a nearly barrier-free exergonic step (**2** → **3-cp**) and a relatively low energy barrier endergonic step (**3-cp** → **4**). The H transfer between the partners within the radical-neutral

https://doi.org/10.52111/qnjs.2022.16301

molecule complex is analogous to the H transfer within an ion molecule complex, which has been previously described because rotation/movement of the partners in the complex is allowed.[140] The low barrier of 13 kcal/mol for the latter step is consistent with recent report of H abstraction from uracil by OH radical that proceeds with a low barrier of about 10 kcal/mol.[141] The overall energy barrier of the reaction chain **2** → 3-**cp** → **4** is only 8 kcal/mol, much smaller than the barrier of the 1,3-H rearrangement **2** → **4**. The OH loss of **4** leading to 2-imino-acetonitrile **5** has relative high energy barrier of 22 kcal/mol. The reaction is endergonic by an amount of 23 kcal/mol.

An exergonic addition of H radical to **5** leads to **6** with a small energy barrier of 4 kcal/mol (cf. Figure 1). Addition of a H radical to a neutral molecule has been previously described in photolytic reactions.[133] Addition of FM to the radical **6** leads to the adduct **7** with a rather low energy barrier of 14 kcal/mol. The multistep H-rearrangement reaction **7** → **8-cp** → **9** again shows a low energy barrier of **8** kcal/mol, as compared to the energy barrier of 22 kcal/mol of the one-step reaction **7** → **9**.

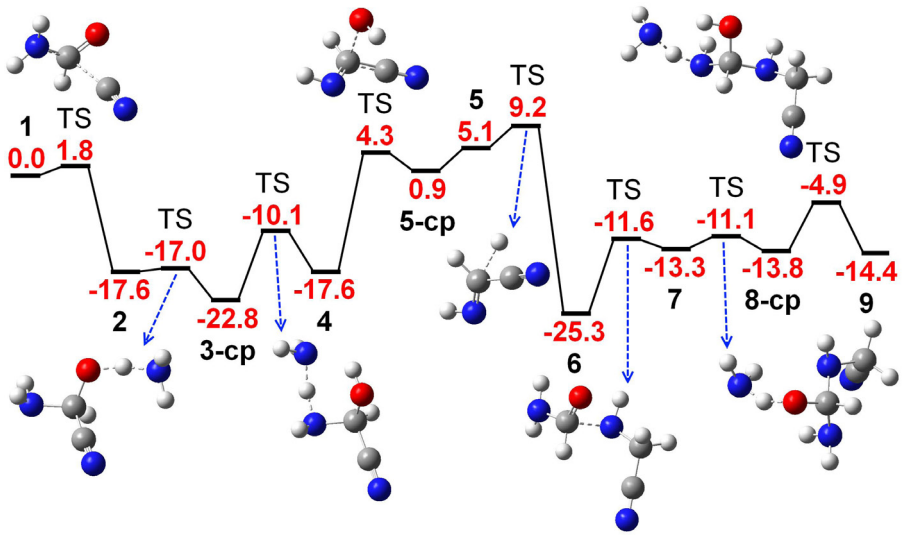

Figure 1. Potential energy profile for the formation of the precursor **9.** Relative energies given in kcal/mol are computed using total energies obtained from geometry optimizations with ZPE corrections at the (U)B3LYP/6-311G(d,p) level.

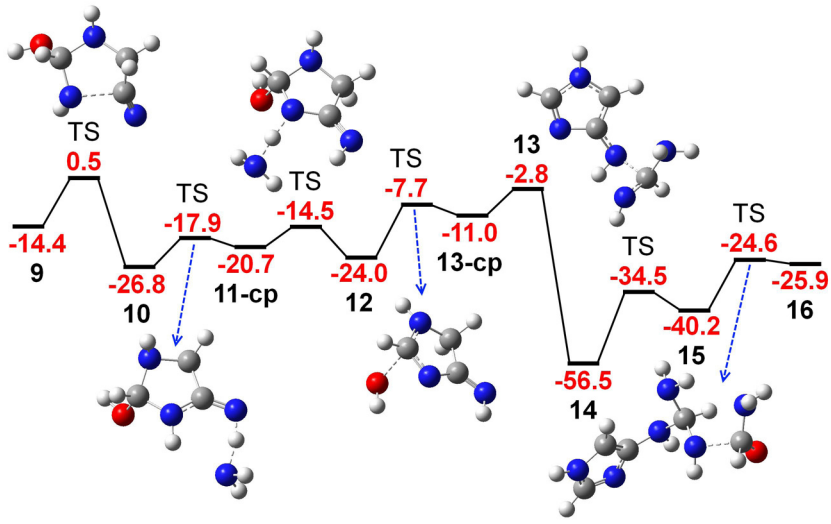

Figure 2. Potential energy profile for the formation of the precursor **16.** Relative energies given in kcal/mol are computed using total energies obtained from geometry optimizations with ZPE corrections at the (U)B3LYP/6-311G(d,p) level.

An intramolecular free radical attack on the triple bond of the CN group in **9** gives rise to a five-membered ring in **10** (cf. Scheme 43). This type of radical attack at the triple bond of the CN group leading to a cyclic structure with an exo-cyclic C=N bond was already reported.[131] Such a cyclization reaction from **9** to **10** is associated with a low energy barrier of 15 kcal/mol, and it is exergonic with a change in energy of –12 kcal/mol (cf. Figure 2). The cyclization of **9** to **10** is a significant improvement over previously reported pathways in forming five-membered rings prebiotically. Cyclization leading to a five-membered ring involving different pathways was recently described as the rate-determining step with an energy barrier of 42 kcal/mol in the presence of water.[89] Accordingly, involvement of free radicals looks realistic for formation of a five-membered ring.

A multistep H rearrangement of **10** leads to **12** with the radical centered on the nitrogen atom of the five-membered ring. Based on previous studies of radical reactions at C=N bond,[134] the role of C=N bond is emphasized. The first step of this multistep reaction is the transfer of H radical to C=N● with an energy barrier of 9 kcal/mol, and the resulting C=NH is targeted for the formation of the six-membered ring of the nucleobases. An endergonic OH radical removal of **12** gives **13** with an energy barrier of 16 kcal/mol and a reaction energy of 21 kcal/mol.

In general, the reaction pathway leading to the formation of **13** from FM shows that these reactions proceed through significantly lower energy barriers than previously reported.[89-90] The neutral species **13** is reactive towards free radicals and it constitutes a prebiotic precursor for purine nucleobases.

The route to purine nucleobases involves the construction of a six-membered ring. The first step of the formation of the precursor **16** is the activation of the neutral precursor **13** to generate a reactive radical **14**, which is stabilized by resonance as indicated by curved arrows in Scheme 4. Activation of **13** with ●CN in this step is highly exergonic and barrier-free (cf. Figure 2). Both the addition of formamidine to **14** leading to **15** and the addition of FM to **15** leading to **16** involve the radical attack of ●NH to the double bonds and are endergonic reactions. These reactions require considerable activation energies of 22 and 16 kcal/mol, respectively. The radical species **16** has two functional groups that can be removed to form the correct functionality in the desired nucleobases, the OH (formed from H addition to the oxygen-centered radical) and the NH_2 groups. Removal of the former yields purine and adenine and removal of the latter yields guanine and hypoxanthine.

3.2. Formation of the purine 26 and adenine 29

Scheme 5 shows the pathways toward production of purine and adenine. Similar to the rearrangement of **2** to **4**, multistep H-radical rearrangement from N to O of **16** leads to **18** followed by the removal of ●OH to give **19**. An exergonic addition of H-radical to **19** gives **20** without an energy barrier followed by a slightly exergonic cyclization from **20** to **21**.

The cyclization step has a low energy barrier of 11 kcal/mol (cf. Figure 3). Again, these results of low energy barrier cyclizations demonstrate the advantage of using free radical mechanisms in the formation of nucleobases. Loss of an H-radical leads to the neutral intermediate 22 with an energy requirement of 40 kcal/mol. The sequential reactions from neutral species **19** to neutral species **22** are cyclization routes with a stepwise addition and elimination of a H radical.

https://doi.org/10.52111/qnjs.2022.16301

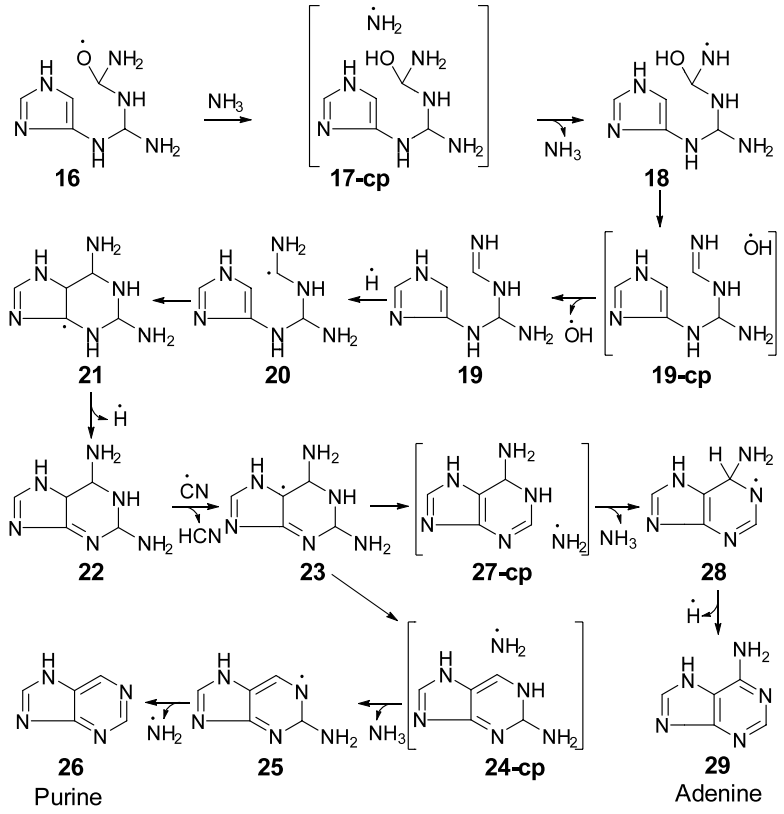

Scheme 5. Formation of purine **26** and adenine **29**

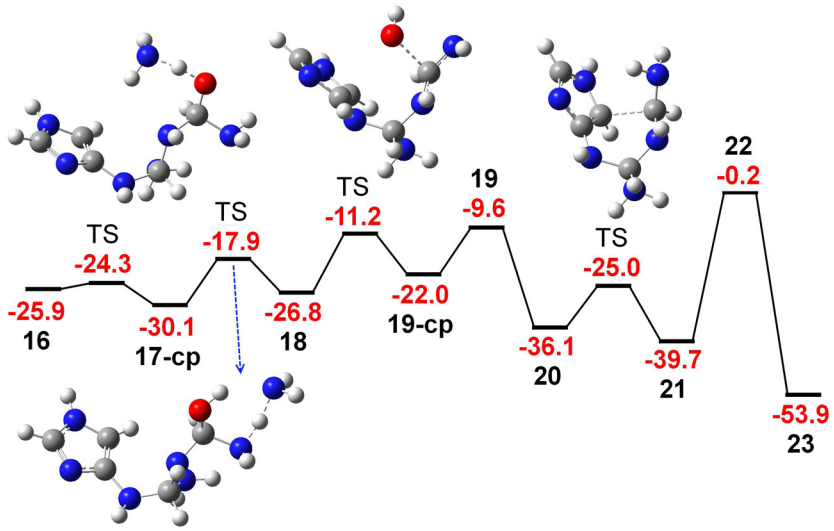

Figure 3. Potential energy profile leading to the formation of **23.** Relative energies given in kcal/mol are computed using total energies obtained from geometry optimizations with ZPE corrections at the (U)B3LYP/6-311G(d,p) level.

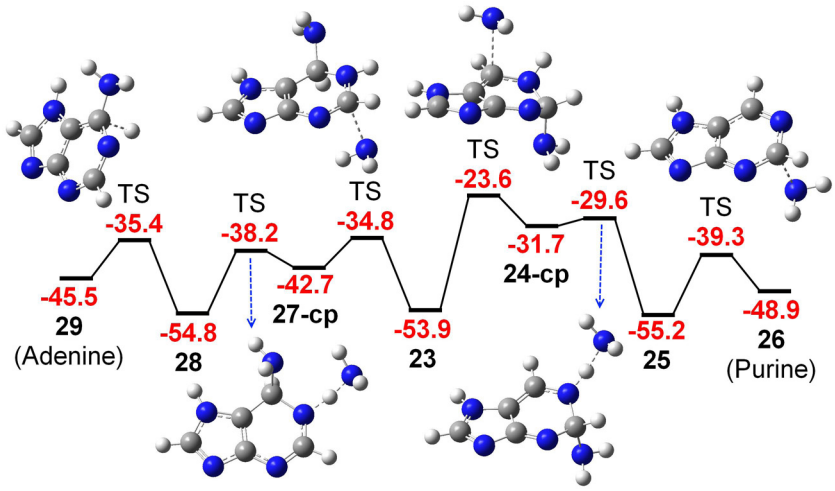

Figure 4. Potential energy profiles leading to the formation of purine **26** and adenine **29.** Relative energies given in kcal/mol are computed using total energies obtained from geometry optimizations with ZPE corrections at the (U)B3LYP/6-311G(d,p) level.

The radical **23** is the precursor for both purine and adenine. The barrier-free step from **22** → **23** (cf. Figure 3) shows that ●CN/HCN pair, similar to ●NH_2/NH_3 pair, can be used to activate neutral precursors toward nucleobase formation. The effect of free radicals to activate neutral intermediates is identified throughout the entire mechanisms. The use of ●CN/HCN leads to a highly exergonic reaction from **22** to **23**.

Figure 4 shows the potential energy profile of the three-step reaction chains from **23** leading to the formation of purine **26** and adenine **29**. The synthesis of purine from **23** consists of a reaction step (**23** → **24-cp**) with a relatively high energy barrier of 30 kcal/mol and two lower energy barrier steps. Meanwhile, the energy barriers for the reaction steps from **23** to adenine are in the range of 5 − 19 kcal/mol.

3.3. Mechanisms for formation of guanine 35 and hypoxanthine 36

The reaction pathways leading to the synthesis of guanine and hypoxanthine and the corresponding potential energy profiles are plotted in Scheme 6 and Figure 5, respectively. Loss of ●NH_2 from 16 yields a radical-neutral molecule complex 30-cp that is energetically favorable. The ●NH_2 subsequently abstracts a H atom from the neutral molecule (**30-cp** → **31**) with a small energy barrier of 6 kcal/mol. Reaction pathways involving radical-neutral molecule complexes are thus feasible for abiotic synthesis.

The cyclization to form the six-membered ring from **31** to give **32** requires **35** kcal/mol and is barrier-free. This energy requirement is still lower than the previously reported energy barriers of 38 and 60 kcal/mol for a similar cyclization step with and without water as a catalyst, respectively.[90]

The mechanisms found here are in agreement with previous findings that the use of free radicals significantly decreases energy barriers of the reactions (by ~30 kcal/mol).[137] The cyclization steps in previous studies had high energy requirements and were prohibitive steps for nucleobase formation. An energy barrier of 32 kcal/mol has been reported for production of a six-membered ring.[89] The route considered by these authors involves an intramolecular cycloaddition step that is appropriate for thermal reactions when free radicals are not involved in the pathways. On the other hand, the current study fits well with several scenarios including non-thermal and non-equilibrium conditions with production of large quantities of radicals.

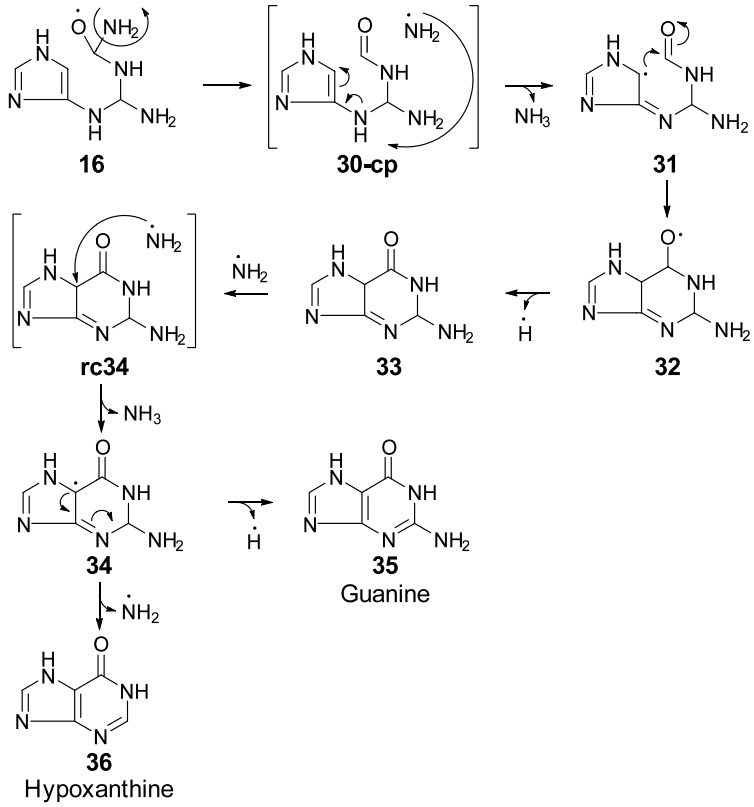

Scheme 6. Formation of guanine **35** and hypoxanthine **36.**

Loss of an H-radical from **32** to give the neutral intermediate **33** shows that the reaction pathway generates reactive radicals, H radical in this case, which can further activate a new cycle of the mechanism. The H transfer reaction within the radical-neutral complex **rc34** leading to **34** has a very low energy barrier of 2 kcal/mol. This reaction step can in fact be considered as a barrier-free reaction because the energy barrier is smaller than the common error of the calculation method. Finally, loss of a H radical leads to guanine **35** and loss of an $\bullet NH_2$ from 34 leads to hypoxanthine **36**. The reactive species generated from these reactions can initiate a new cycle for the production of nucleobases. It should be noted that production of guanine and hypoxanthine shares one pathway from the beginning with the difference appearing only in the last step.

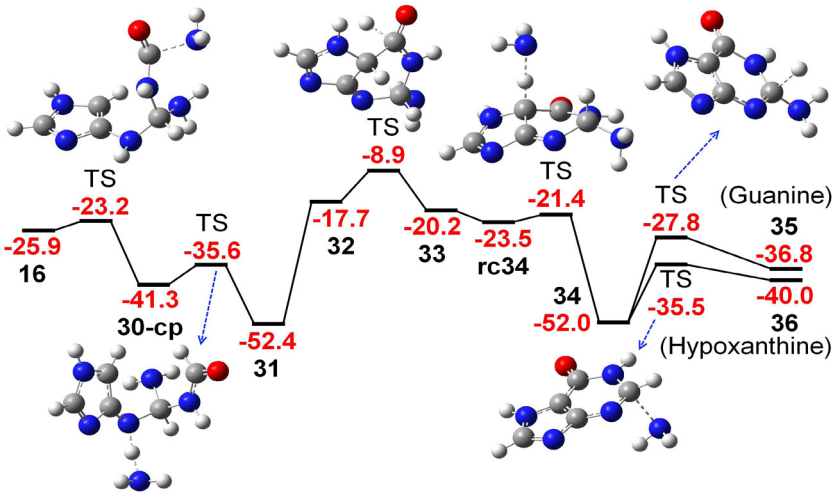

Figure 5. Potential energy profiles leading to the formation of guanine **35** and hypoxanthine **36,** Relative energies given in kcal/mol are computed using total energies obtained from geometry optimizations with ZPE corrections at the (U)B3LYP/6-311G(d,p) level.

3.4. Mechanisms for formation of xanthine 48

The precursor **40** of xanthine and isoguanine is formed from the radical imidazol derivative **14** (cf. Scheme 7 and Figure 6). To account for the number of heavy atoms (C, O and N) in xanthine and isoguanine, addition of two molecules of FM to **14** is required. The first step is a radical addition of **14** to FM to give **37** with an energy barrier of 25 kcal/mol, followed by the low-barrier multistep H rearrangement **37** → **38-cp** → **39**. This H shift is necessary for N to become part of the heterocycle. Addition of another molecule of FM to **39** yields **40** with a lower energy barrier of 14 kcal/mol as compared to that of the **14** → **37** addition step.

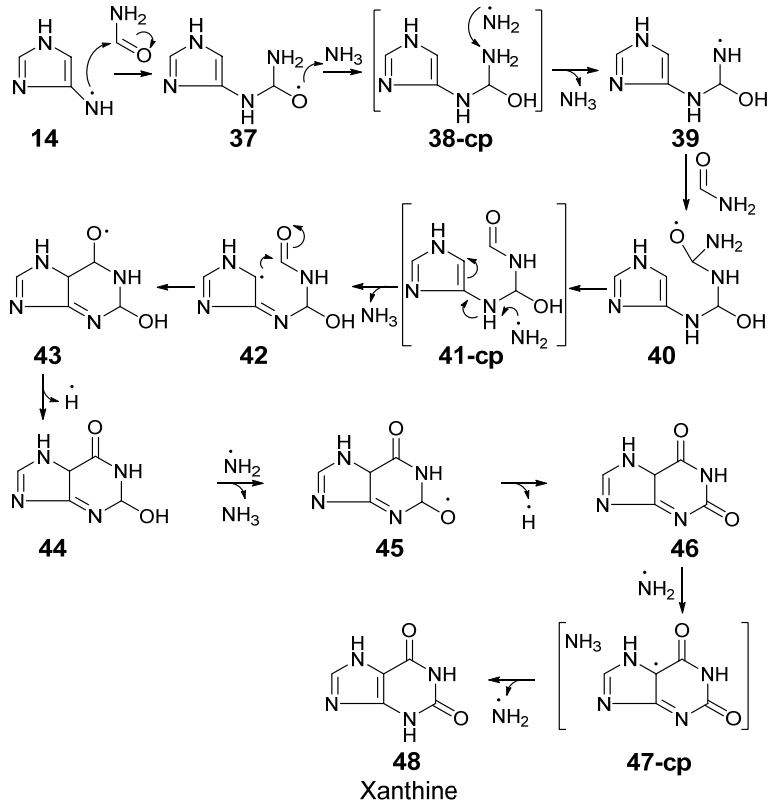

Scheme 7. Formation of xanthine **48**

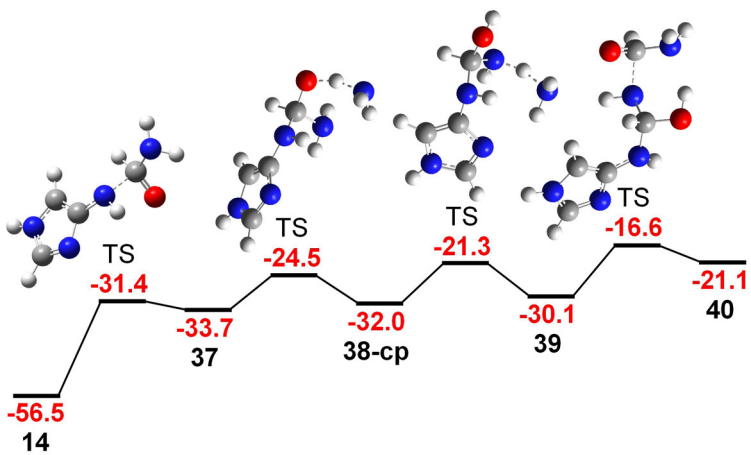

Figure 6. Potential energy profile leading to the formation of **40**. Relative energies given in kcal/mol are computed using total energies obtained from geometry optimizations with ZPE corrections at the (U)B3LYP/6-311G(d,p) level.

https://doi.org/10.52111/qnjs.2022.16301

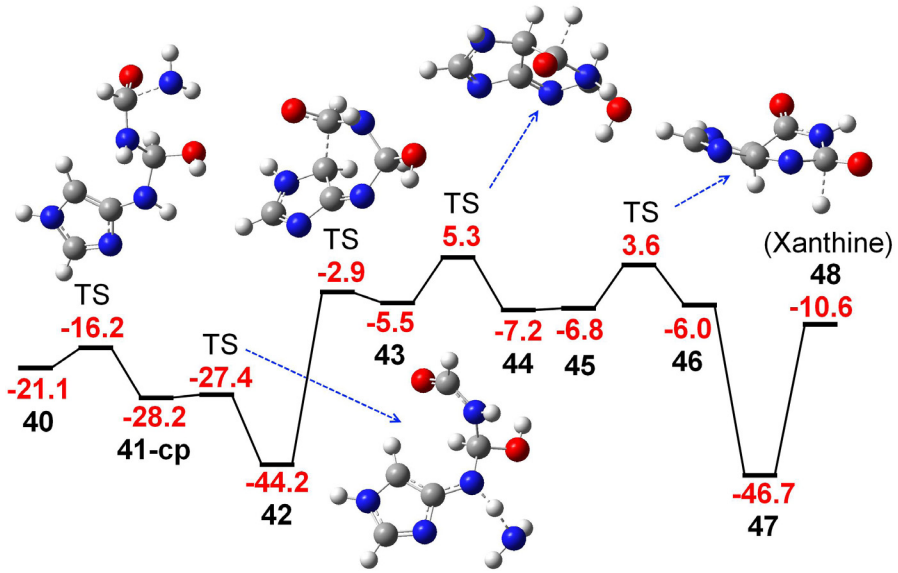

Figure 7. Potential energy profile leading to the formation of xanthine **48.** Relative energies given in kcal/mol are computed using total energies obtained from geometry optimizations with ZPE corrections at the (U)B3LYP/6-311G(d,p) level.

Figure 7 shows the potential energy profile of the formation of xanthine from **40**. Elimination of a $\bullet NH_2$ radical from **40** gives rise to the formation of the radical-molecule complex **41-cp**. Hydrogen abstraction by the $\bullet NH_2$ results in **42** with a very small energy barrier of 1 kcal/mol. Again, this reaction step can be considered as a barrier-free reaction. The radical cyclization of **42** to **43** requires a high activation energy of 41 kcal/mol, the highest activation barrier within the current mechanism. This step is highly endergonic with a reaction energy of 39 kcal/mol.

The remaining steps to xanthine constitute the two carbonyl groups in the six-membered rings. Mechanisms leading to the formation of carbonyl groups are important in prebiotic chemistry due to the fact that a facile formation of carbonyl group may lead to the functional group transformations required for the construction of complex molecules. The first carbonyl group is simply formed by abstracting a H radical from the H−C−O● of **43** to form **44**. This reaction has a low energy barrier of 11 kcal/mol. Sequential loss of two H atoms from the hydroxyl group of **44** forms the remaining carbonyl group in the six-membered ring of **46**. The first H loss is assisted by NH_2 radical and is barrier-free, whereas the second H loss has an energy barrier of 3 kcal/mol. The multistep 1,3-H radical rearrangement from 46 gives xanthine 48. Both elementary steps in this process are barrier-free. The H abstraction by NH_2 (46 → 47-cp) is exergonic and the H addition by NH_3 (47-cp → 48) is endergonic.

3.5. Mechanisms for formation of isoguanine 58

Because of structural similarity, a mechanism leading to xanthine is expected to also generate isoguanine. The latter requires elimination of a ●OH from **40** while xanthine requires elimination of $\bullet NH_2$. Therefore, the starting of isoguanine mechanisms is a low-energy-barrier multistep 1,3-H shift from **40** to form **50** (cf. Scheme 8).

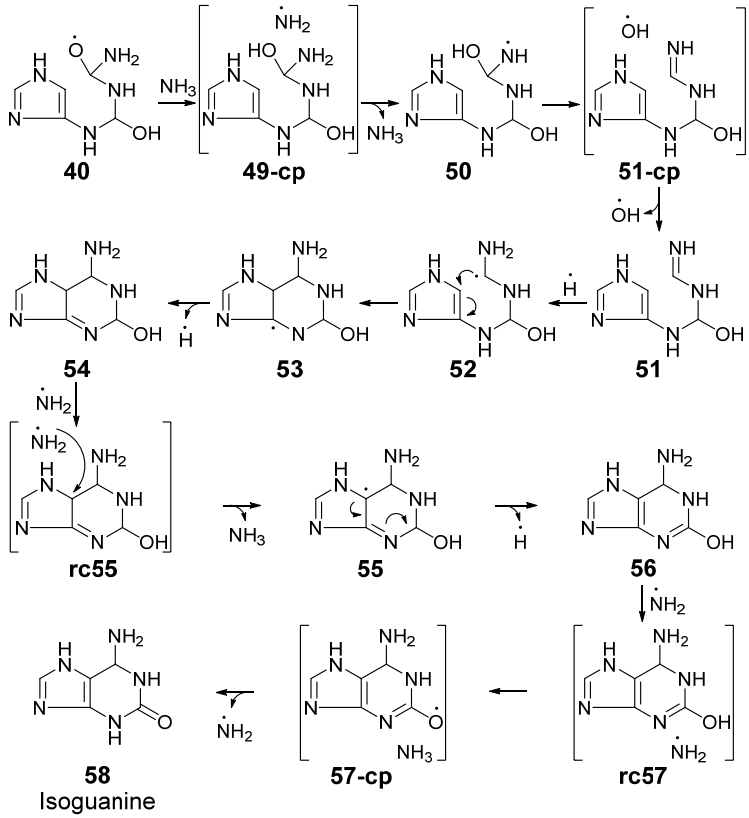

Scheme 8. Formation of isoguanine **58**

Endergonic loss of •OH from **50** produces the neutral intermediate **51** with a reaction energy of 17 kcal/mol (cf. Figure 8). A two-step radical cyclization reaction can thus be proposed. The first step of the cyclization is the barrier-free addition of a •H to **51** to give **52**. Cyclization of **52** gives **53** with an energy barrier of 20 kcal/mol. This channel shows a relatively lower barrier than the previously reported one for the non-catalyzed cyclization step. However, a H loss from **53** to form **54** has a high energy barrier of 45 kcal/mol.

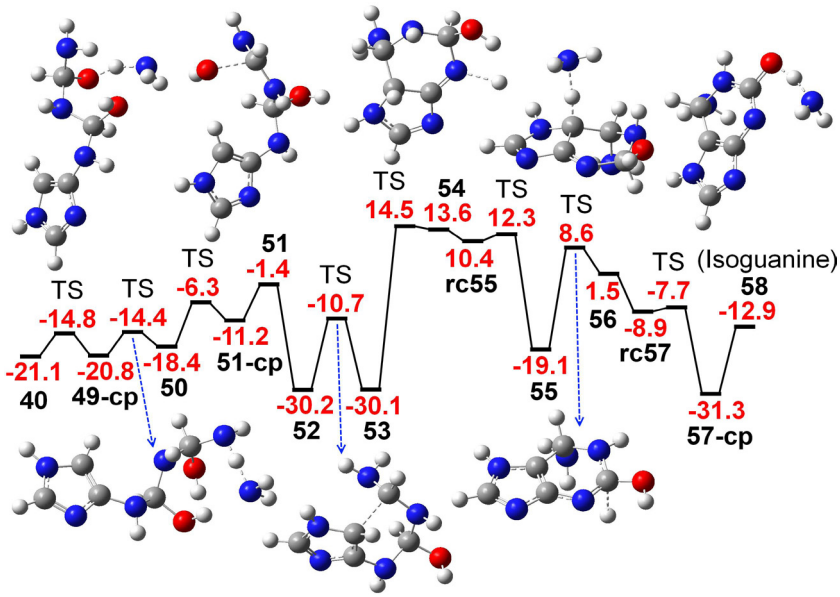

Figure 8. Potential energy profile leading to the formation of isoguanine **58.** Relative energies given in kcal/mol are computed using total energies obtained from geometry optimizations with ZPE corrections at the (U)B3LYP/6-311G(d,p) level.

https://doi.org/10.52111/qnjs.2022.16301

Similar to the xanthine pathways, loss of two hydrogens from **54** forms the enol of isoguanine. This channel involves $\bullet NH_2$ for the abstraction of a hydrogen atom from **54** to **55**. A H loss from **55** yields **56** which is the enol of isoguanine **58**. The energy barrier for the **55** → **56** step amounts to 28 kcal/mol. Again, similar to xanthine, formation of isoguanine **58** from the tautomerizations of **56** can take place with the presence of the $\bullet NH_2/NH_3$ pair. The overall tautomerization process is exergonic by an amount of 14 kcal/mol.

3.6. Formation of cytosine 71

Both the five-membered ring of purines and the six-membered ring of pyrimidines can be formed from the nitrogen-centered radical **9** (cf. Scheme 3). The purine ring is simply formed by intramolecular radical attack of ●NH group on the C≡N triple bond as mentioned above ($\Delta E^{\#}$ = 15 kcal/mol).

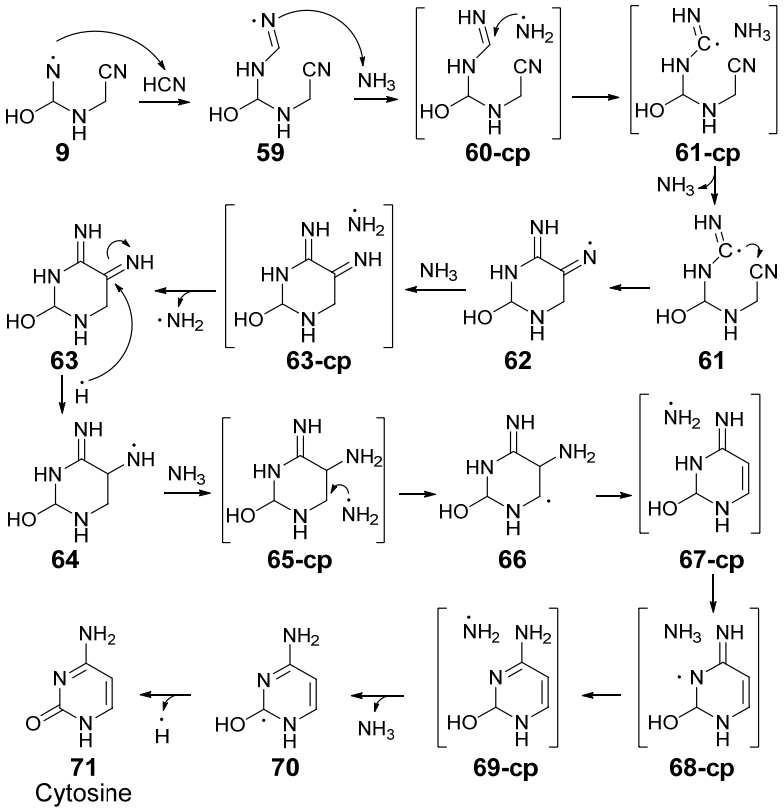

Scheme 9. Formation of cytosine **71**

It is obvious from structure of **9** that an extra carbon atom is needed to complete the chemical frame of pyrimidine ring. This can be done by adding an HCN molecule to **9** via an intermolecular free radical attack on the C≡N bond to form the nitrogen-centered radical **59** as presented in Scheme 9.

This pathway is consistent with a previous suggestion that cytosine is formed from two FM and two HCN molecules, even not under Titan condition.[143-146] Note that two FM and one HCN molecules have been consumed to form **9** (cf. Scheme 3). This radical-attack-CN reaction, even though it has the same nature as the purine ring formation from **9**, has a much lower energy barrier ($\Delta E\#$ = 8 cal/mol). In both cases, the conversion of the CN triple to double bond releases energy and thus makes the reaction exergonic. The energy release of the reaction **9** → **59** is –14 kcal/mol. The potential energy profiles and the involving transition structures of the reaction pathway from the radical intermediate **9** to cytosine **71** are plotted in Figures 6.9 and 6.10. The role of the C≡N as energy reservoir due to the large amount of bond energy released from its partial bond breaking has previously been suggested.[96]

The sp_2-imino carbon-centered radical **61** is formed from **59** via the $\bullet NH_2/NH_3$-assisted H rearrangement. This overall H rearrangement is slightly endergonic by 7 kcal/mol with a relatively low energy barrier of 10 kcal/mol. The next step is the intramolecular radical cyclization of **61** in which the highly reactive sp_2 carbon-centered radical attacks the C≡N bond forming the cyclic species **62**. Again, this reaction is exergonic by an amount of -11 kcal/mol upon a partial breaking of the C≡N bond. In addition, this ring closure step has lower energy barrier ($\Delta E^{\#}$: 7 kcal/mol) than the purine five-membered ring formation.

The next reaction steps from **62** to **66** are a series of H radical additions (**62** → **63**, **63** → **64**) and rearrangements (**64** → **65-cp** → **66**). These steps are necessary for the subsequent removal of the NH_2 group (**66** → **67-cp**). Although the H-addition step **62** → **63** is endergonic by an amount of 16 kcal/mol, the relatively large amount of energy release from the addition of an H atom to **63** and the subsequent H rearrangement makes the whole reaction chain from **62** to **66** exergonic with the net energy release of –21 kcal/mol. These reactions have relatively low energy barriers ($\Delta E\# = 5 - 14$ kcal/mol, cf. Figures 9 and 10).

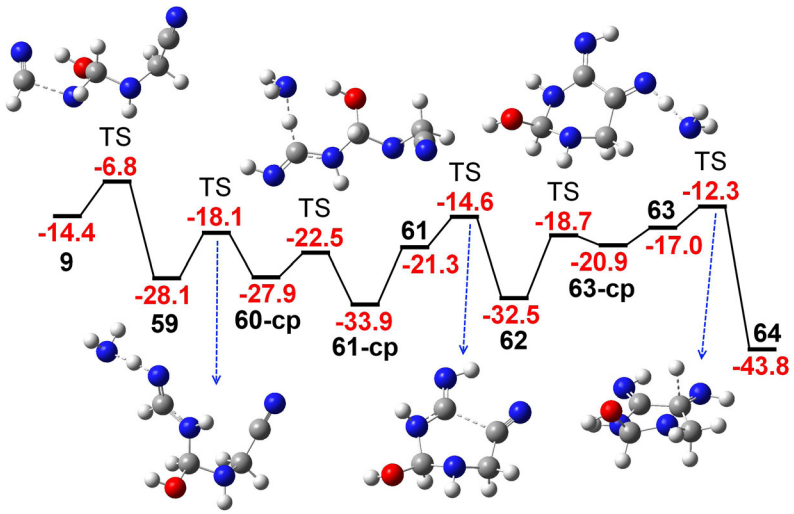

Figure 9. Potential energy profile leading to the formation of **64.** Relative energies given in kcal/mol are computed using total energies obtained from geometry optimizations with ZPE corrections at the (U)B3LYP/6-311G(d,p) level.

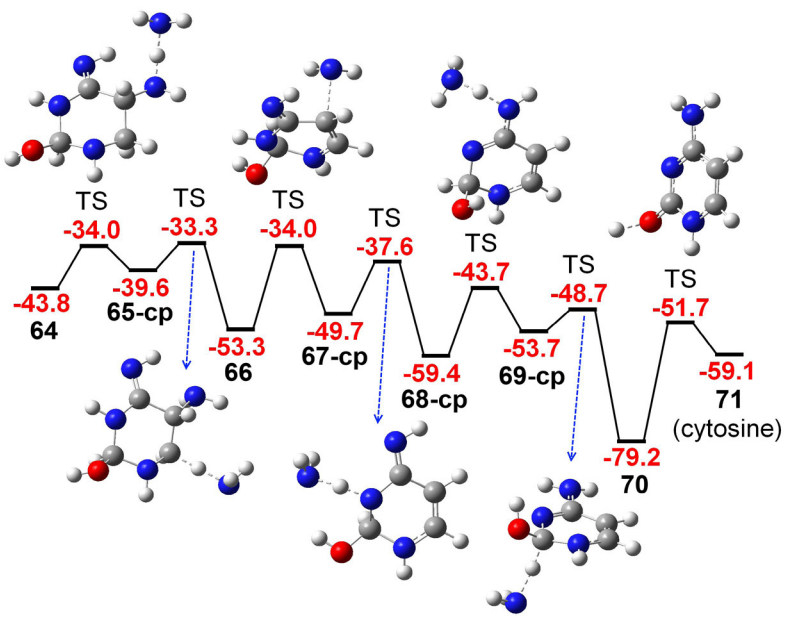

Figure 10. Potential energy profile leading to the formation of cytosine **7.** Relative energies given in kcal/mol are computed using total energies obtained from geometry optimizations with ZPE corrections at the (U)B3LYP/6-311G(d,p) level.

https://doi.org/10.52111/qnjs.2022.16301

The release of NH_2 radical from **66** forms the $^5C=^6C$ double bond of cytosine ring within the complex **67-cp**. This reaction has an energy barrier of 19 kcal/mol. All three pyrimidines use the same numbering system which is indicated in Scheme 2. The subsequent H rearrangement (**67-cp** → **70**) includes three elementary steps: the H- abstraction at 3N position of **67-cp**, H-addition to the external NH group at 4C position of **68-cp**, and H-abstraction at 2C position of **69-cp**. This rearrangement reaction is exergonic by –29 kcal/mol and a relatively low overall energy barrier of 12 kcal/mol. A final H loss from **70** forms cytosine **71**. This reaction involves a high overall energy barrier of 28 kcal/mol and is endergonic by 20 kcal/mol. Nevertheless, the pathway leading to cytosine from FM is still highly exergonic with the net gain in energy of –59 kcal/mol.

3.7. Formation of uracil 75

Formation of uracil from cytosine is presented in Scheme 10. The enol tautomer **73** of uracil is formed from cytosine by replacing the NH_2 substituent by OH group. This substituent replacement takes place via two steps including the addition of OH radical to the 4C position and the elimination of more stable NH_2 radical. The potential energy profile and the transition structures of this route are plotted in Figure 11 with the relative energy of cytosine taken from the route in Figure 10. Both steps have low energy barriers with the second step being exergonic by 19 kcal/mol. The NH_2 radical in the radical-neutral complex **73-cp** facilitates the enol-keto tautomerization leading to a slightly more stable keto form **76** of uracil. The complex of uracil and NH_2 radical **75-cp1** is also presented here because it is involved in the formation of thymine (discussed in a following section). Formation of uracil from FM and HCN in this main route is thermodynamically feasible with an overall gain in energy of –81 kcal/mol.

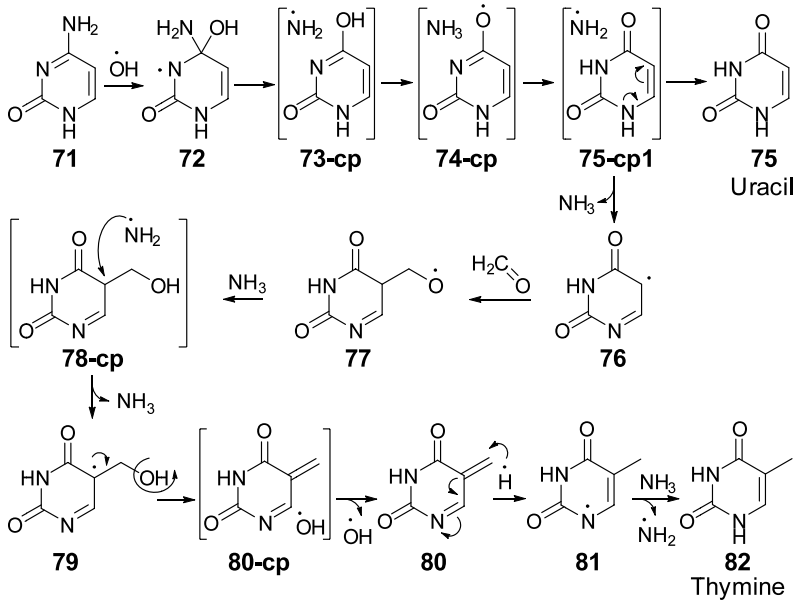

Scheme 10. Formation of uracil **75** and thymine **82**

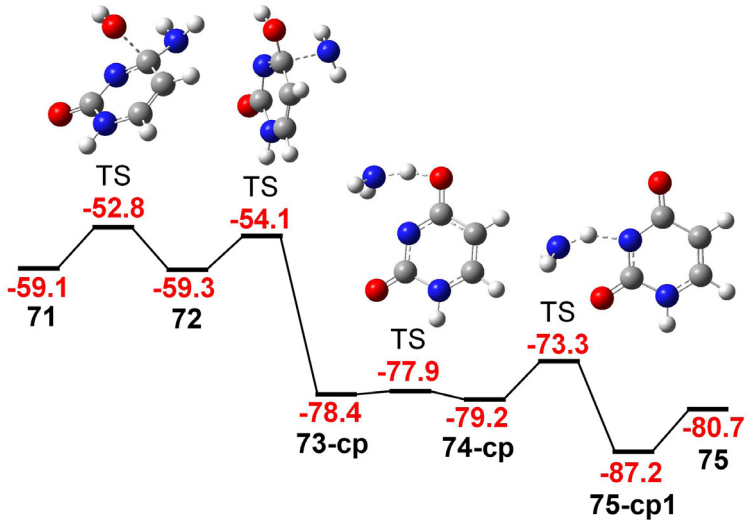

Figure 11. Potential energy profile leading to the formation of uracil **75.** Relative energies given in kcal/mol are computed using total energies obtained from geometry optimizations with ZPE corrections at the (U)B3LYP/6-311G(d,p) level.

3.8. Formation of thymine 82

Thymine can be formed from uracil by replacing the H atom at the 5C position by a CH_3 group. This methyl substituent can be added using one-carbon compounds available in the reaction mixture.

In the mechanism yielding thymine from the uracil complex **75-cp1** presented in Scheme 10 and Figure 12, H loss at 1N position of uracil generates the nitrogen-centered radical **76**. The conjugated form of **76** with the radical center located at the 5C atom (sp_3) can subsequently react with $H_2C{=}O$ yielding the oxygen-centered radical of 5-hydroxymethyluracil **77**. The next H-rearrangement step **77** → **78-cp** → **79** gives the carbon-centered radical of 5-hydroxymethyluracil **79**, which is much more stable than the oxygen-centered radical **77**. The following OH loss **79** → **80** is however highly endergonic with an absorbed energy of 40 kcal/mol.

The two-step radical hydrogenation turns the methylene group in the neutral product **80** into the methyl group of thymine **82**. The large amount of energy released from the first H-addition step **80** → **81** compensates the energy taken in the previous steps, and thus makes this whole reaction chain exergonic by –104 kcal/mol.

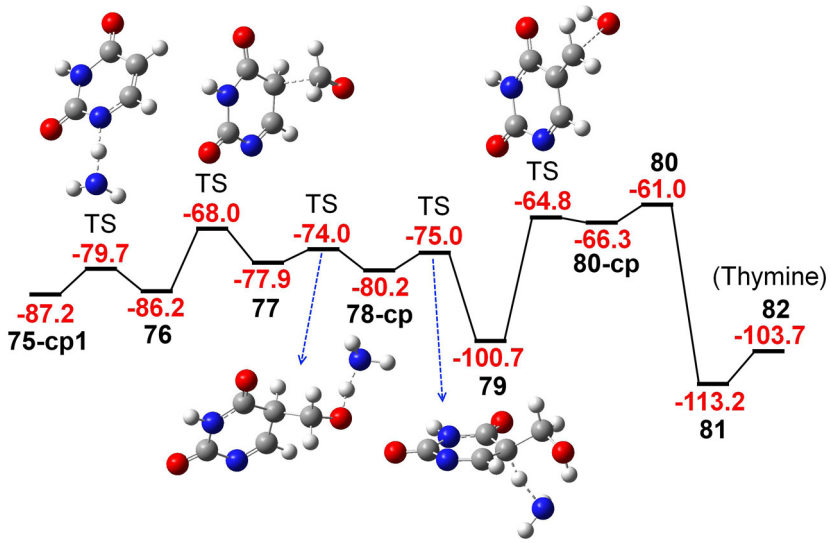

Figure 12. Potential energy profile leading to the formation of thymine **82.** Relative energies given in kcal/mol are computed using total energies obtained from geometry optimizations with ZPE corrections at the (U)B3LYP/6-311G(d,p) level.

https://doi.org/10.52111/qnjs.2022.16301

3.9. Effect of temperature on the free radical mechanisms

The enthalpy barriers, enthalpies of reactions, Gibbs free energy barriers and Gibbs free energies of reactions at 94 K being the surface temperature of Titan, 298 K the commonly used standard ambient temperature, and 483 K being the boiling point of FM, are calculated to investigate the effect of temperature on the suggested mechanisms. Energy, enthalpy and Gibbs free energy profiles of the reaction pathways leading to the formation of adenine **29**, guanine **35**, cytosine **71**, uracil **75**, and thymine **82** are plotted in Figures 13 and 14 in black, blue, and red, respectively. The three profiles are close together at low temperature but the differences increase at higher temperatures. It is obvious that the variation of the Gibbs free energy profiles is much more profound than that of the enthalpy profiles.

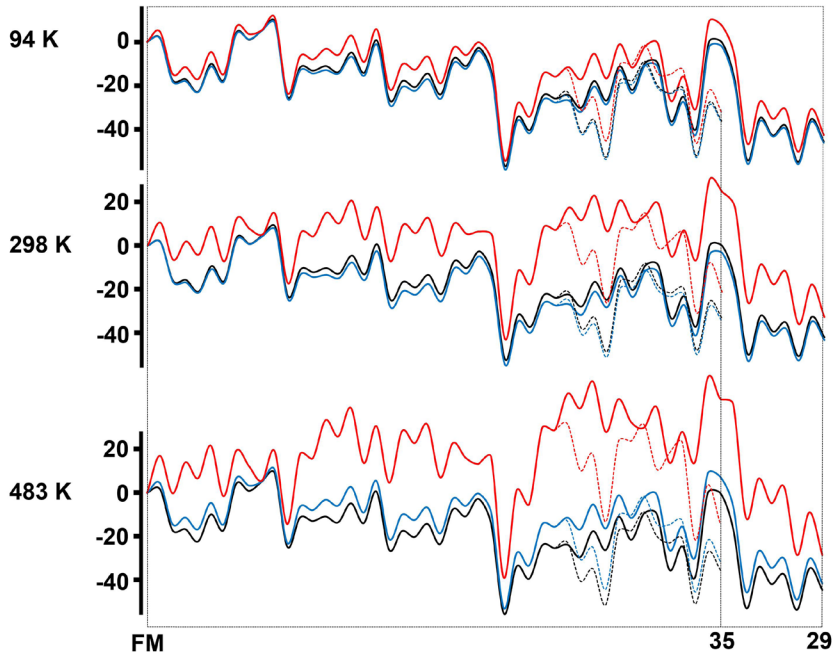

Figure 13. Energy, enthalpy and Gibbs free energy profiles (kcal/mol, in black, blue, and red, respectively) of the reaction pathways leading to the formation of adenine **29** and guanine **35** (UB3LYP/6-311G(d,p))

Table 3. Overall energy barriers and reaction energies ($\Delta E^{\#}$, ΔE_R), enthalpy barriers and enthalpies of reaction ($\Delta H^{\#}$, ΔH_R), and Gibbs free energy barriers and Gibbs free energies of reaction ($\Delta G^{\#}$, ΔG_R) in kcal/mol of the main routes leading to the formation of adenine **29**, guanine **35**, cytosine **71**, uracil **75** and thymine **82** from FM.

	$\Delta E^{\#}$	94 K		298 K		483 K	
		$\Delta H^{\#}$	$\Delta G^{\#}$	$\Delta H^{\#}$	$\Delta G^{\#}$	$\Delta H^{\#}$	$\Delta G^{\#}$
1 → 29	9.3	8.5	11.0	7.7	32.6	7.0	53.8
1 → 35	9.3	8.5	11.0	7.7	22.2	7.0	39.8
1 → 71							
1 → 75	9.3	8.5	11.0	7.7	22.2	7.0	44.4
1 → 82							
	ΔE_R	ΔH_R	ΔG_R	ΔH_R	ΔG_R	ΔH_R	ΔG_R
1 → 29	-45.5	-46.1	-42.5	-46.9	-35.5	-47.6	-29.1
1 → 35	-36.2	-36.8	-32.2	-37.6	-23.1	-38.3	-14.8
1 → 71	-59.0	-61.8	-54.4	-64.7	-41.2	-67.2	-29.2
1 → 75	-80.6	-83.2	-76.2	-86.0	-63.7	-88.6	-52.4
1 → 82	-103.6	-106.5	-96.6	-109.7	-78.3	-112.6	-61.8

The overall energy, enthalpy, Gibbs free energy barriers ($\Delta E^{\#}$, $\Delta H^{\#}$, and $\Delta G^{\#}$), and the overall reaction energies (ΔE_R), enthalpies of reactions (ΔH_R) and Gibbs free energies of reactions (ΔG_R) of these reaction pathways are given in Table 3. The data show obviously unfavourable changes of the overall $\Delta G^{\#}$ and ΔG_R upon increasing temperature. Although the reaction mechanisms become less exergonic as the temperature increase, the overall ΔG_R values for the formation of adenine, guanine, cytosine, uracil and thymine at 483 K remain negative, being –29, –15, –29, –52, and –62 kcal/mol, respectively. Our calculations show that the overall ΔG_R change sign from negative to positive at the temperatures of ~1300, ~800, ~900, ~1300 and ~1200 K for the formation of adenine, guanine, cytosine, uracil, and thymine, respectively.

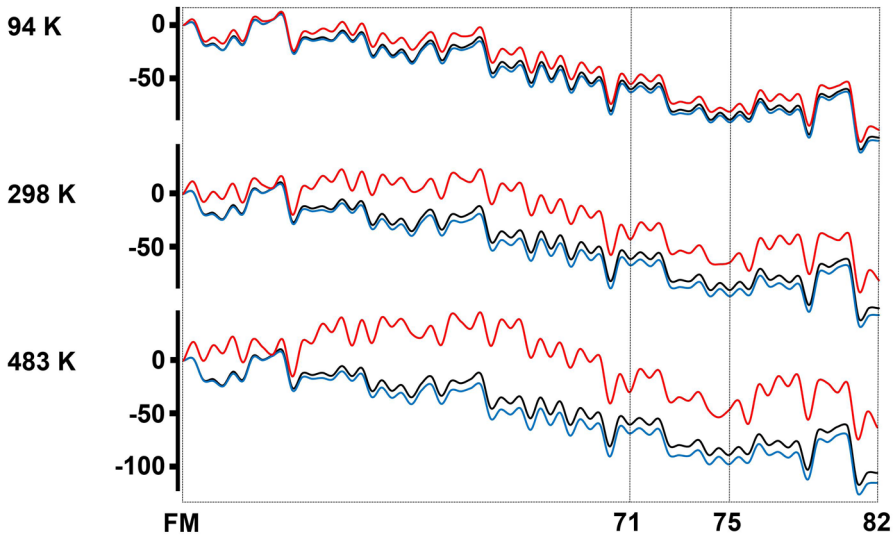

Figure 14. Energy, enthalpy and Gibbs free energy profiles (kcal/mol, in black, blue, and red, respectively) of the reaction pathways leading to the formation of cytosine **71**, uracil **75**, and thymine **82** (UB3LYP/6-311G(d,p)).

4. CONCLUDING REMARKS

In this paper, we reviewed the results obtained by quantum chemical computations with the aim to probe the free radical routes leading to formation of DNA nucleobases from formamide. The mechanisms identified here demonstrate that important nucleobases can be formed under conditions consistent with the nitrogen-rich atmosphere such as Titan, regardless of whether water is present or absent.

Laboratory simulation experiments of the extra-terrestrial conditions are not trivial to setup because of the limited knowledge of the unseen environment. However, increasing synthetic and spectral evidence for organic compounds have been found in the organic haze of Titan's atmosphere. Formation of complex molecules under such environments can be expected to proceed in part through free radical pathways.

The free radicals constitute promising routes for the nonthermal construction of biomolecules. They further promote our understanding in the prebiotic synthesis of heterocyclic organic compounds. All of the suggested mechanisms in the present work employed simple radical reactions such as H-shifts, $\bullet$H/$\bullet$OH/$\bullet NH_2$ radical losses, and most importantly intramolecular radical 1,n-cyclization. The advantages of free radical mechanisms are the inherently low energy barriers that are observed in most reaction steps and the highly exergonic nature of the whole reaction chains. The channels lead to more than one product at the end, which brings in the concept of diversity in biomolecules formed from a single prebiotic route. In addition, the mechanisms discovered here can be used to explain the non-terrestrial origin of xanthine, as previously suggested.[104]

https://doi.org/10.52111/qnjs.2022.16301

The pathways for xanthine and isoguanine pointed out that more compounds should also be expected, because of the emergence of stable neutral intermediates along the ways. However, other entrance channels on the potential energy surface such as the coupling of two radicals should also be taken into consideration since they are expected to reduce the yields of nucleobases.

Acknowledgements

The authors are grateful to the KU Leuven Research Council for support.

REFERENCES

1. P. S. Cohen, S. M. Cohen. Wöhler's synthesis of urea: how do the textbooks report it?, *Journal of Chemical Education*, **1996**, *73*, 883.
2. S. L. Miller. A production of amino acids under possible primitive earth conditions, *Science*, **1953**, *117*, 528.
3. S. L. Miller, H. C. Urey. Organic compound synthesis on the primitive earth, *Science*, **1959**, *130*, 245.
4. C. U. Lowe, M. W. Rees, R. F. R. S. Markham. Synthesis of complex organic compounds from simple precursors: formation of amino-acids, amino-acid polymers, fatty acids and purines from ammonium cyanide, *Nature*, **1963**, *199*, 219.
5. A. Voet, A. Schwartz. Uracil is released from HCN oligomers, *Origins Life and Evolution of Biospheres*, **1982**, *12*, 45.
6. J. Oró. Synthesis of adenine from ammonium cyanide, *Biochemical Biophysical Research Communicaions*, **1960**, *2,* 407.
7. J. Oró, A. P. Kimball. Synthesis of purines under possible primitive earth conditions. I. Adenine from hydrogen cyanide, *Archives of Biochemistry and Biophysics*, **1961**, *94*, 217.
8. A. Ricardo, M. A. Carrigan, A. N. Olcott, S. A. Benner. Borate minerals stabilize ribose, *Science*, **2004**, *303*, 196.
9. H. Lin, E. I. Jimanez, J. T. Arriola, U. F. Muller, R. R. Krrisnamirthy. Concurrent prebiotic formation of nucleoside-amidophosphates and nucleoside-triphosphates potentiates transition from abiotic to biotic polymerization, *Angewandte Chemie International Edition,* **2022**, *61*, e202113625.
10. M. W. Powner, B. Gerland, J. D. Sutherland. Synthesis of activated pyrimidine ribonucleotides in prebiotically plausible conditions, *Nature*, **2009**, *459*, 239.
11. J. Oró, S. S. Kamat. Amino-acid synthesis from hydrogen cyanide under possible primitive earth conditions, *Nature*, **1961**, *190*, 442.
12. J. Jortner. Conditions for the emergence of life on the early Earth: summary and reflections, *Philosophical Transactions of the Royal Society B: Biological Sciences*, **2006**, *361*, 1877.
13. N. Aylward, N. Bofinger. The reactions of methanimine and cyanogen with carbon monoxide in prebiotic molecular evolution on earth, *Origins of Life and Evolution of the Biosphere*, **2001**, *31,* 481.
14. K. Kobayashi, T. Kaneko, C. Ponnamperuma, T. Oshima, H. Yanagawa, T. Saito. Abiotic synthesis of bioorganic compounds in simulated primitive planetary environments, *Nippon Kagaku Kaishi*, **1997**, 823.
15. D. M. Rank, C. Townes, W. J. Welch. Interstellar molecules and dense clouds, *Science*, **1971**, *174*, 1083.
16. P. Ehrenfreund, S. B. Charnley. Organic molecules in the interstellar medium, comets, and meteorites: a voyage from dark clouds to the early Earth, *Annual Review of Astronomy and Astrophysics*, **2000**, *38*, 427.
17. M. De Becker, F. Raucq. Catalogue of particle-accelerating colliding-wind binaries, *Astronomy & Astrophysics*, **2013**, *558*, 33.
18. K. Kvenvolden, J. Lawless, K. Pering, E. Peterson, J. Flores, C. Ponnamperuma, C. Moore. Evidence for extraterrestrial amino-acids and hydrocarbons in the Murchison meteorite, *Nature*, **1970**, *28*, 923.

19. Y. J. Kuan, S. B. Charnley, H. C. Huang, W. L. Tseng, Z. Kisiel. Interstellar glycine, *The Astrophysical Journal*, **2003**, *593*, 848.

20. Z. Martins, O. Botta, M. L. Fogel, M. A. Sephton, D. P. Glavin, J. S. Watson, P. Ehrenfreund. Extraterrestrial nucleobases in the Murchison meteoritel, *Earth and Planetary Science Letters*, **2008**, *270*, 130.

21. R. Saladino, C. Crestini, G. Costanzo, R. Negri, E. Di Mauro. A possible prebiotic synthesis of purine, adenine, cytosine, and 4 (3H)-pyrimidinone from formamide: implications for the origin of life, *Bioorganic & Medicinal Chemistry*, **2001**, *9*, 1249.

22. K. O. Stetter. Hyperthermophiles in the history of life, *Philosophical Transactions of the Royal Society B: Biological Sciences*, **2006**, *361*, 1837.

23. S. L. Miller, A. Lazcano. The origin of life—did it occur at high temperatures?, *Journal of Molecular Evolution*, **1995**, *41,* 689.

24. S. Islas, A. M. Velasco, A. Becerra, L. Delaye, A. Lazcano. Hyperthermophily and the origin and earliest evolution of life, *International Microbiology*, **2003**, *6*, 87.

25. A. W. Schwartz, H. Joosten, A. B. Voet. Prebiotic adenine synthesis via HCN oligomerization in ice, *Biosystems*, **1982**, *15*, 191.

26. H. J. Cleaves II, K. E. Nelson, S. L. Miller. The prebiotic synthesis of pyrimidines in frozen solution, *Naturwissenschaften*, **2006**, *93*, 228.

27. S. Miyakawa, H. J. Cleaves, S. L. Miller. The cold origin of life: B. Implications based on pyrimidines and purines produced from frozen ammonium cyanide solutions, *Origins Life and Evolution of Biospheres,* **2002**, *32*, 195.

28. M. Levy, S. L. Miller, K. Brinton, J. L. Bada. Prebiotic synthesis of adenine and amino acids under Europa-like conditions, *Icarus*, **2000**, *145*, 609.

29. M. P. Robertson, M. Levy, S. L. Miller. Prebiotic synthesis of diaminopyrimidine and thiocytosine, *Journal of Molecular Evolution*, **1996**, *43*, 543.

30. M. Colin-Garcia, A. Heredia, A. Negron-Mendoza, F. Ortega, T. Pi, S. Ramos-Bernal. Adsorption of HCN onto sodium montmorillonite dependent on the pH as a component to chemical evolution, *International Journal of Astrobiology*, **2014**, *13*, 310.

31. M. Colín-García, F. Ortega-Gutiérrez, S. Ramos-Bernal, A. Negrón-Mendoza. Heterogeneous radiolysis of HCN adsorbed on a solid surface, *Nuclear Instruments and Methods in Physics Research Section A: Accelerators, Spectrometers, Detectors and Associated Equipment*, **2010**, *619*, 83.

32. J. D. Bernal. The physical basis of life, *Proceedings of the Physical Society A,* **1949,** *62*, 537.

33. M. Paecht-Horowitz. Clays as possible catalysts for peptide formation in the prebiotic era, *Origins of Life*, **2010**, *7,* 369.

34. I. Hashizume. Role of clay minerals in chemical evolution and the origins of life, *Clay Minerals in Nature—Their Characterization, Modification and Application*, **2012**.

35. M. Franchi, E. Bramanti, L. M. Bonzi, P. L. Orioli, C. Vettori, E. Gallori. Clay-nucleic acid complexes: characteristics and implications for the preservation of genetic material in primeval habitats, *Origins of Life and Evolution of the Biosphere*, **1999**, *29*, 297.

36. G. Wächtershäuser. Before enzymes and templates: theory of surface metabolism, *Microbiological Reviews*, **1988**, *52*, 452.

37. G. Wächtershäuser. Pyrite formation, the first energy source for life: a hypothesis, *Systematic and Applied Microbiology*, **1988**, *10*, 207.

38. G. Wächtershäuser. Life as we don't know it, *Science*, **2000**, *289*, 1307.

39. G. F. Joyce. The antiquity of RNA-based evolution, *Nature*, **2002**, *418*, 214.

40. R. Saladino, C. Crestini, S. Pino, G. Costanzo, E. Di Mauro. Formamide and the origin of life, *Physics of Life Reviews*, **2012,** *9*, 84.

41. J. P. Ferris, P. C. Joshi. Chemical evolution from hydrogen cyanide: photochemical decarboxylation of orotic acid and orotate derivatives, *Science*, **1978**, *201*, 361.

https://doi.org/10.52111/qnjs.2022.16301

42. R. Saladino, C. Crestini, F. Ciciriello, G. Costanzo, E. Di Mauro. About a formamide-based origin of informational polymers: syntheses of nucleobases and favourable thermodynamic niches for early polymers, *Origins of Life and Evolution of Biospheres*, **2006**, *36*, 523.

43. G. R. Adande, N. J. Woolf, L. M. Ziurys. Observations of interstellar formamide: Availability of a prebiotic precursor in the galactic habitable zone, *Astrobiology*, **2013**, *13*, 439.

44. R. A. Sanchez, J. P. Ferbis, L. E. Orgel. Studies in prebiodc synthesis: II. Synthesis of purine precursors and amino acids from aqueous hydrogen cyanide, *Journal of Molecular Biology*, **1967**, *30*, 223.

45. D. Bockelee-Morvan, D. C. Lis, J. E. Wink, D. Despois, J. Crovisier, R. Bachiller, D. J. Benford, N. Biver, P. Colom, J. K. Davies, E. Gerard, B. Germain, M. Houde, D. Mehringer, R. Moreno, G.Paubert, T.G. Phillips, H. Rauer. *Astronony Astrophysics,* **2000**, *353,* 1101.

46. D. Bockelée-Morvan, D. C. Lis, J. E. Wink, D. Despois, J. Crovisier, R. Bachiller, H. Rauer. New molecules found in comet C/1995 O1 (Hale-Bopp). Investigating the link between cometary and interstellar material, *Astronomy and Astrophysics*, **2000,** *353*, 1101.

47. P. Schilke, C. Comito, S. Thorwirth, F. Wyrowski, K. M. Menten, R. Güsten, L. A. Nyman. Submillimeter spectroscopy of southern hot cores: NGC 6334 (I) and G327.3-0.6, *Astronomy & Astrophysics*, **2006**, *454*, L41.

48. J. C. Boden, R. A. Back. Photochemistry and free-radical reactions in formamide vapour, *Transactions of the Faraday Society*, **1970**, *66*, 175-182.

49. T. Kakumoto, K. Saito, A. Imamura. Thermal decomposition of formamide: shock tube experiments and ab initio calculations, *Journal of Physical Chemistry*, **1985**, *89*, 2286.

50. J. Lundell, M. Krajewska, M. Räsänen. Matrix isolation fourier transform infrared and ab initio studies of the 193-nm-induced photodecomposition of formamide, *Journal of Physical Chemistry A*, **1998**, *102*, 6643.

51. T. Y. Kang, H. L. Kim. Photodissociation of formamide at 205 nm: The H atom channels, *Chemical Physics Letters*, **2006**, *431*, 24.

52. F. Cataldo, G. Patane, G. Compagnini. Synthesis of HCN polymer from thermal decomposition of formamide, *Journal of Macromolecular Science, Part A: Pure and Applied Chemistry*, **2009**, *46*, 1039.

53. S. D. Senanayake, H. Idriss. Photocatalysis and the origin of life: Synthesis of nucleoside bases from formamide on TiO_2 (001) single surfaces, *Proceedings of the National Academy of Sciences*, **2006**, *103*, 1194.

54. Y. J. Chen, M. Nuevo, C. C. Chu,Y. G. Fan, T. S. Yih, W. H. Ip, C. Y. Wu. Photo-desorbed species produced by the UV/EUV irradiation of an H_2O: CO_2: NH_3 ice mixture, *Advances in Space Research*, **2011,** *47*, 1633.

55. S. Jheeta, A. Domaracka, S. Ptasinska, B. Sivaraman, N. J. Mason. The irradiation of pure CH_3OH and 1: 1 mixture of NH_3: CH_3OH ices at 30 K using low energy electrons, *Chemical Physics Letters*, **2013**, *556*, 359.

56. C. A. Tsipis, P. A. Karipidis. Mechanistic insights into the Bazarov synthesis of urea from NH_3 and CO_2 using electronic structure calculation methods, *Journal of Physical Chemistry A,* **2005**, *109*, 8560.

57. R. Saladino, U. Ciambecchini, C. Crestini, G. Costanzo, R. Negri, E. Di Mauro. One-pot TiO_2-catalyzed synthesis of nucleic bases and acyclonucleosides from formamide: Implications for the origin of life, *ChemBioChem*, **2003**, *4*, 514.

58. M. Okazaki, T. Funazukuri. Decomposition of acetamide and formamide in pressurized hot water, *Journal of Materials Science*, **2006**, *41*, 1517.

59. A. Butlerow. Complexes of ribose with silicates, borates, and calcium: Implications to Astrobiology, *Comptes Rendus de l'Academie des Sciences,* **1961**, *53*, 145.

60. G. Springsteen, G. F. Joyce. Selective derivatization and sequestration of ribose from a

prebiotic mix, *Journal of the American Chemical Society*, **2004**, *126*, 9578.

61. H. H. J. Cleaves. The prebiotic geochemistry of formaldehyde, *Precambrian Research*, **2008**, *164*, 111.

62. T. McCollom, G. Ritter, B. T. Simoneit. An important origin of life scenario involving molecular replication is the RNA-world, *Origins Life and Evolution of Biospheres,* **1999**, *29*, 153.

63. H. Yamada, T. Okamoto. Polycyclic N-hetero compounds. XIV. Reactions of methylpyridines with formamide, *Chemical Pharmaceutical Bulletins,* **1972**, *20*, 623.

64. R. Saladino, C. Crestini, U. Ciambecchini, F. Ciciriello, G. Costanzo, E. Di Mauro. Synthesis and degradation of nucleobases and nucleic acids by formamide in the presence of montmorillonites, *ChemBioChem*, **2004**, *5*, 1558.

65. R. Saladino, C. Crestini, V. Neri, J. R. Brucato, L. Colangeli, F. Ciciriello, G. Costanzo. Synthesis and degradation of nucleic acid components by formamide and cosmic dust analogues, *ChemBioChem*, **2005**, *6*, 1368.

66. R. Saladino, C. Crestini, V. Neri, F. Ciciriello, G. Costanzo, E. Di Mauro. Origin of informational polymers: The concurrent roles of formamide and phosphates, *ChemBioChem*, **2006**, *7*, 1707.

67. R. Saladino, V. Neri, C. Crestini, G. Costanzo, M. Graciotti, E. Di Mauro. Synthesis and degradation of nucleic acid components by formamide and iron sulfur minerals, *Journal of the American Chemical Society*, **2008**, *130*, 15512.

68. R. Barks, R. Buckley, G. A. Grieves, E. Di Mauro, N. V. Hud, T. M. Orlando. Guanine, adenine, and hypoxanthine production in UV-irradiated formamide solutions: relaxation of the requirements for prebiotic purine nucleobase formation, *ChemBioChem*, **2010**, *11*, 1240.

69. S. Sedaghat, J. M. Leveque, M. Draye. Amino-acid synthesis in aqueous media under ultrasonic irradiation, *Chemistry of Natural Compounds*, **2010**, *46,* 75.

70. R. Saladino, V. Neri, C. Crestini, G. Costanzo, M. Graciotti, E. Di Mauro. The role of the formamide/zirconia system in the synthesis of nucleobases and biogenic carboxylic acid derivatives, *Journal of Molecular Evolution*, **2010**, *71*, 100.

71. R. Saladino, C. Crestini, C. Cossetti, E. Di Mauro, D. Deamer. Catalytic effects of Murchison material: Prebiotic synthesis and degradation of RNA precursors, *Origins of Life and Evolution of Biospheres*, **2011**, *41*, 437.

72. R. Saladino, J. R. Brucato, A. De Sio, G. Botta, E. Pace, L. Gambicorti. Photochemical synthesis of citric acid cycle intermediates based on titanium dioxide, *Astrobiology*, **2011**, *11*, 815.

73. U. Shanker, B. Bhushan, G. Bhattacharjee. Formation of nucleobases from formamide in the presence of iron oxides: Implication in chemical evolution and origin of life, *Astrobiology*, **2011**, *11*, 225.

74. R. Saladino, M. Barontini, C. Cossetti, E. Di Mauro & C. Crestini. The effects of borate minerals on the synthesis of nucleic acid bases, amino acids and biogenic carboxylic acids from formamide, *Origins of Life and Evolution of Biospheres*, **2011**, *41*, 317.

75. R. Saladino, G. Botta, M. Delfino, E. Di Mauro. Meteorites as catalysts for prebiotic chemistry, *Chemistry–A European Journal*, **2013**, *19*, 16916.

76. A. Kumar, R. Sharma. Formamide-based synthesis of nucleobases by metal (II) octacyanomolybdate (IV): implication in prebiotic chemistry, *Astrobiology*, **2014**, *14*, 769.

77. M. Ferus, R. Michalcikova, V. Shestivská, J. Sponer, J. E. Sponer, S. Civis. High-energy chemistry of formamide: A simpler way for nucleobase formation, *Journal of Physical Chemistry A*, **2014**, *118*, 719.

78. M. Ferus, D. Nesvorný, J. Šponer, P. Kubelík, R. Michalčíková, V. Shestivská, S. Civiš. High-energy chemistry of formamide: A unified mechanism of nucleobase formation, *Proceedings of the National Academy of Sciences*, **2015**, *112*, 657.

https://doi.org/10.52111/qnjs.2022.16301

79. Y. L. Yung, M. Allen, J. P. Pinto. Photochemistry of the atmosphere of Titan: comparison between model and observations, *Astrophysical Journal, Supplement S,* **1984**, *55,* 465.

80. M. S. Gudipati, R. Jacovi, I. Couturier-Tamburelli, A. Lignell, M. Allen. Photochemical activity of Titan's low-altitude condensed haze, *Nature Communications,* **2013**, *4,* 1648.

81. S. Pilling, D. P. P. Andrade, A. C. Neto, R. Rittner, A. N. de Brito. DNA Nucleobase Synthesis at Titan Atmosphere Analog by Soft X-rays, *Jounal of Physical Chemistry A,* **2009**, *113*, 11161.

82. M. Nuevo, S. N. Milam, S. A. Sandford. Nucleobases and prebiotic molecules in organic residues produced from the ultraviolet photo-irradiation of pyrimidine in NH_3 and H_2O-NH_3 ices, *Astrobiology*, **2012**, *12*, 295.

83. E. Camprubí, J.W. de Leeuw, C.H. House, F. Raulin, M.J. Russell, A. Spang, M. R. Tirumalai, F. Westall. The emergence of life, *Space Science Review*, **2019**, 215.

84. S. M. Hörst, R. V. Yelle, A. Buch, N. Carrasco, G. Cernogora, O. Dutuit, V. Vuitton. Formation of amino acids and nucleotide bases in a Titan atmosphere simulation experiment, *Astrobiology*, **2012**, *12*, 809.

85. R. Shapiro. Prebiotic cytosine synthesis: a critical analysis and implications for the origin of life, *Proceedings of the National Academy of Sciences*, **1999**, *96*, 4396.

86. J. E. Šponer, A. Mládek, J. Šponer, M. Fuentes-Cabrera. Formamide-based prebiotic synthesis of nucleobases: a kinetically accessible reaction route, *Journal of Physical Chemistry A*, **2012**, *116*, 720.

87. V. S. Nguyen, H. L. Abbott, M. M. Dawley, T. M. Orlando, J. Leszczynski, M. T. Nguyen. Theoretical study of formamide decomposition pathways, *Journal of Physical Chemistry A*, **2011**, *115*, 841.

88. V. S. Nguyen, T. M. Orlando, J. Leszczynski, M. T. Nguyen. Theoretical study of the decomposition of formamide in the presence of water molecules, *Journal of Physical Chemistry A*, **2013**, *117*, 2543.

89. J. Wang, J. Gu, M. T. Nguyen, G. Springsteen, J. Leszczynski. From formamide to purine: An energetically viable mechanistic reaction pathway, *Journal of Physical Chemistry B*, **2013**, *117*, 2314.

90. J. Wang, J. Gu, M. T. Nguyen, G. Springsteen, J. Leszczynski. From formamide to purine: A self-catalyzed reaction pathway provides a feasible mechanism for the entire process, *Journal of Physical Chemistry B*, **2013**, *117*, 9333.

91. J. Wang, J. Gu, M. T. Nguyen, G. Springsteen, J. Leszczynski. From formamide to adenine: a self-catalytic mechanism for an abiotic approach, *Journal of Physical Chemistry B*, **2013**, *117*, 14039.

92. D. Roy, K. Najafian, P. von Ragué Schleyer. Chemical evolution: The mechanism of the formation of adenine under prebiotic conditions, *Proceedings of the National Academy of Sciences*, **2007**, *104*, 17272.

93. H. T. Nguyen, M. T. Nguyen. Effects of sulfur-deficient defect and water on rearrangements of formamide on pyrite (100) surface, *Journal of Physical Chemistry A*, **2014**, *118*, 4079.

94. H. T. Nguyen, M. T. Nguyen. Effects of water molecules on rearrangements of formamide on the kaolinite basal (001) surface, *Journal of Physical Chemistry A*, **2014**, *118*, 7017.

95. H. T. Nguyen, V. S. Nguyen, N. T. Trung, R. W. Havenith, M. T. Nguyen. Decomposition pathways of the neutral and protonated formamide in some lower-lying excited states, *Journal of Physical Chemistry A*, **2013**, *117*, 7904.

96. M. Ferus, S. Civis, A. Mládek, J. Šponer, L. Juha, J. E. Šponer. On the road from formamide ices to nucleobases: IR-spectroscopic observation of a direct reaction between cyano radicals and formamide in a high-energy impact event, *Journal of the American Chemical Society*, **2012**, *134*, 20788.

97. V. P. Gupta, P. Rawat, R. N. Singh, P. Tandon. Formation of 2-imino-malononitrile and diaminomaleonitrile in nitrile rich environments: A quantum chemical study, *Computational and Theoretical Chemistry*, **2012**, *983*, 7.

98. V. P. Gupta, P. Tandon, P. Mishra. Some new reaction pathways for the formation of cytosine in interstellar space. A quantum chemical study, *Advances in Space Research*, **2013**, *51*, 797.

99. A. Landera, A. M. Mebel. Low-temperature mechanisms for the formation of substituted azanaphthalenes through consecutive CN and C_2H additions to styrene and N-methylenebenzenamine: a theoretical study, *Journal of the American Chemical Society*, **2013**, *135*, 7251.

100. P. A. Gerakines, M. H. Moore, R. L. Hudson. Ultraviolet photolysis and proton irradiation of astrophysical ice analogs containing hydrogen cyanide, *Icarus*, **2004**, *170*, 202.

101. J. S. Hudson, J. F. Eberle, R. H. Vachhani, L. C. Rogers, J. H. Wade, R. Krishnamurthy, G. Springsteen. A unified mechanism for abiotic adenine and purine synthesis in formamide, *Angewandte Chemie*, **2012**, *124*, 5224.

102. G. Costanzo, R. Saladino, C. Crestini, F. Ciririello, E. Di Mauro. Nucleoside phosphorylation by phosphate minerals, *BMC Evolutionary Biology,* **2007**, *7*, 1471.

103. R. Saladino, V. Neri, C. Crestini. The philosophy of life: Vitalism and spontaneous generation, *Philosophical Magazine,* **2020**, *90*, 2329.

104. G. Mitri, A. P. Showman, J. I. Lunine, R. D. Lorenz. Hydrocarbon lakes on Titan, *Icarus*, **2007**, *186*, 385.

105. L. Nejdl, L. Petera, J. Sponer, K. Zemankova, K. Pavelicova, A. Knızek, V. Adam, M. Vaculovicova, O. Ivanek, M. Ferus. Quantum dots in peroxidase-like chemistry and formamide-based hot spring synthesis of nucleobases, *Astrobiology*, **2022**, *22*, 541.

106. E. Dushanov, Kh. Khomurodov, K. Tasuoka. Toward an integration of IteD1-response theory and cognitive error diagnosis, *Open Biochemistry Journal,* **2013**, *7*, 33.

107. R. Saladino, G. Botta, B. M. Bizzarri, E. Di Mauro, J. M. Garcia Ruiz. A global scale scenario for prebiotic chemistry: Silica-based self-assembled mineral structures and formamide, *Biochemistry*, **2016**, *55*, 2806.

108. R. Saladino, L. Botta, E. Di Mauro. The prevailing catalytic role of meteorites in formamide prebiotic processes, *Life*, **2018**, *8*, 6.

109. L. Botta, R. Saladino, B. M. Bizzarri, B. Cobucci-Ponzano, Rz. Iacono, R. Avino, S. Caliro, A. Carandente, F. Lorenzini, A. Tortora, E. Di Mauro, M. Moracci. Photo-oxidative behavior of PP/GnP nanocomposites, *Advances in Space Research,* **2018**, *62*, 2372.

110. S. Slavova, V. Enchev. Self-catalytic mechanism of prebiotic reactions: From formamide to purine bases, *International Journal of Quantum Chemistry*, **2020**, *120*, e26362.

111. V. Enchev, S. Slavova. Self-catalytic mechanism of prebiotic reactions: from formamide to pterins and guanine, *Physical Chemistry Chemical Physics*, **2021**, *23*, 19043.

112. S. Slavova, V. Enchev. Self-catalytic mechanism of prebiotic reactions: II. From urea and glycinamide to hypoxanthine, *International Journal of Quantum Chemistry,* **2020**, *120*, e26508.

113. R. Saladino, E. Di Mauro, J. M. García-Ruiz. A universal geochemical scenario for formamide condensation and prebiotic chemistry, *Chemistry, a European Jounal*, **2019**, *25*, 3181.

114. A. Pastorek, M. Ferus, V. Čuba, O. Šrámek, O. Ivanek, S. Civiš. Primordial radioactivity and prebiotic chemical evolution: Effect of γ radiation on formamide-based synthesis, *Journal of Physical Chemistry B*, **2020**, *124*, 8951.

115. V. Enchev, I. Angelov, I. Dincheva, N. Stoyanova, S. Slavova, M. Rangelov, N. Markova. Chemical evolution: from formamide to nucleobases and amino acids without the presence of catalyst, *Journal of Biomolecular Structure and Dynamics*, **2021**, *39*, 5563.

116. L. Petera, K. Mrazikova, L. Nejdl, K. Zemankova, M. Vaculovicova, A. Pastorek, J. Sponer. Prebiotic route to thymine from formamide. A combined experimental–theoretical study, *Molecules*, **2021**, *26*, 2248.

https://doi.org/10.52111/qnjs.2022.16301

117. B. M. Camprubí, R. Saladino, I. Delfino, J. M. García-Ruiz, E. Di Mauro. Prebiotic organic chemistry of formamide and the origin of life in planetary conditions: What we know and what is the future, *International Journal of Molecular Sciences*, **2021**, *22*, 917.

118. T. Das, S. Ghule, K. Vanka. Insights into the origin of life: Did it begin from HCN and H_2O?, *ACS Central Science*, **2019**, *5*, 1532.

119. Y. A. Jeilani, T. M. Orlando, A. Pope, C. Pirim, M. T. Nguyen. Prebiotic synthesis of triazines from urea: a theoretical study of free radical routes to melamine, ammeline, ammelide and cyanuric acid, *RSC Advances*, **2014**, *4*, 32375.

120. Y. A. Jeilani, H. T. Nguyen, B. H. Cardelino, M. T. Nguyen. Free radical pathways for the prebiotic formation of xanthine and isoguanine from formamide, *Chemical Physics Letters*, **2014**, *598*, 58.

121. H. T. Nguyen, Y. A. Jeilani, H. M. Hung, M. T. Nguyen. Radical pathways for the prebiotic formation of pyrimidine bases from formamide, *Journal of Physical Chemistry A*, **2015**, *119*, 8871.

122. Y. A. Jeilani, C. Fearce, M. T. Nguyen. Acetylene as an essential building block for prebiotic formation of pyrimidine bases on Titan, *Physical Chemistry Chemical Physics*, **2015**, *17*, 24294.

123. Y. A. Jeilani, P. N. Williams, S. Walton, M. T. Nguyen. Unified reaction pathways for the prebiotic formation of RNA and DNA nucleobases, *Physical Chemistry Chemical Physics*, **2016**, *18*, 20177.

124. M. Ferus, P. Kubelík, A. Knížek, A. Pastorek, J. Sutherland, S. Civiš. High energy radical chemistry formation of HCN-rich atmospheres on early Earth, *Scientific Reports*, **2017**, *7*, 1.

125. Y. A. Jeilani, B. Ross, N. Aweis, C. Fearce, H. M. Hung, M. T. Nguyen. Reaction routes for experimentally observed intermediates in the prebiotic formation of nucleobases under high-temperature conditions, *Journal of Physical Chemistry A*, **2018**, *122*, 2992.

126. S. Kaur, P. Sharma. Radical pathways for the formation of non-canonical nucleobases in prebiotic environments, *RSC Advances*, **2019**, *9*, 36530.

127. R. W. Lim, A. C. Fahrenbach. Radicals in prebiotic chemistry, *Pure and Applied Chemistry*, **2020**, *92*, 1971.

128. Y. A. Jeilani, M. T. Nguyen. Autocatalysis in formose reaction and formation of RNA nucleosides, *Journal of Physical Chemistry B*, **2020**, *124*, 11324.

129. A. D. Becke. Density-functional exchange-energy approximation with correct asymptotic behavior, *Physical Review A*, **1988**, *38,* 3098.

130. C. T. Lee, W. T. Yang, R. G. Parr. Development of the Colle-Salvetti correlation-energy formula into a functional of the electron density, *Physical Review B,* **1988**, *37*, 785.

131. W. J. Hehre, L. Radom, P. v. R. Schleyer, J. A. Pople. *Ab initio molecular orbital theory*, Wiley Interscience, New York, USA, 1986.

132. J. Wang, J. Gu, J. Leszczynski. Hints from Computational Chemistry: Mechanisms of Transformations of Simple Species into Purine and Adenine by Feasible Abiotic Processes. *Practical aspects of computational chemistry III*, Springer, Germany, 2015, 393-427.

133. A. A. Fokin, P. R. Schreiner. Selective alkane transformations via radicals and radical cations: Insights into the activation step from experiment and theory, *Chemical Reviews*, **2002**, *102*, 1551.

134. D. Moscatelli, M. Dossi, C. Cavallotti, G. Storti. Density functional theory study of addition reactions of carbon-centered radicals to alkenes, *Journal of Physical Chemistry A*, **2011**, *115*, 52.

135. J. P. Ferris, L. E. Orgel. An unusual photochemical rearrangement in the synthesis of adenine from hydrogen cyanide, *Journal of the American Chemical Society*, **1966**, *88*, 1074.

136. B. H. Munk, C. J. Burrows, H. B. Schlegel. Exploration of mechanisms for the transformation of 8-hydroxy guanine radical to FAPyG by density functional theory, *Chemical Research in Toxicology*, **2007**, *20*, 432.

137. R. M. Nelson, L. W. Kamp, D. L. Matson, P. G. Irwin, K. H. Baines, M. D. Boryta, B. Sicardy. Saturn's Titan: Surface change, ammonia, and implications for atmospheric and tectonic activity, *Icarus*, **2009**, *199*, 429.

138. C. Gonzalez, H. B. Schlegel. Atmospheric chemistry of Titan: ab initio study of the reaction between nitrogen atoms and methyl radicals, *Journal of the American Chemical Society*, **1992**, *114*, 9118.

139. H. T. Nguyen, M. T. Nguyen. Decomposition pathways of formamide in the presence of vanadium and titanium monoxides, *Physical Chemistry Chemical Physics*, **2015**, *17*, 16927.

140. Z. Hu, S. D Li, P. Z. Hong. Intramolecular cascade radical cyclizations promoted by samarium diiodide, *Arkivoc*, **2010**, *9*, 171.

141. K. P. Prasanthkumar, C. H. Suresh, C. T. Aravindakumar. Theoretical study of the addition and abstraction reactions of hydroxyl radical with uracil, *Radiation Physics and Chemistry*, **2012**, *81*, 267.

142. M. Pettersson, L. Khriachtchev, S. Jolkkonen, M. Räsänen. Photochemistry of HNCO in solid Xe: channels of UV photolysis and creation of H_2NCO radicals, *Journal of Physical Chemistry A*, **1999**, *103*, 9154.

143. M. Gioanola, R. Leardini, D. Nanni, P. Pareschi, G. Zanardi. Aryl radical cyclisation on to a pyrrole nucleus, *Tetrahedron,* **1995**, *51,* 2039.

144. H. Yamada, M. Hirobe, K. Higashiyama, H. Takahashi, K. T. Suzuki. Reaction mechanism for purine ring formation as studied by 13C-15N coupling, *Tetrahedron Letters*, **1978**, *19*, 4039.

145. T. Wang, J. H. Bowie. Can cytosine, thymine and uracil be formed in interstellar regions? A theoretical study, *Organic & Biomolecular Chemistry*, **2012**, *10*, 652.

146. M. Ferus, A. Knížek, L. Petera, A. Pastorek, J. Hrnčířová L.Jankovič, O. Ivanek, J. Šponer A. Křivková, H. Saeidfirozeh, S. Civiš, E. Chatzitheodoridis, K. Mráziková, M. Nejdl, F. Saija, J. E. Šponer, G. Cassone. Formamide-based Post-impact thermal prebiotic synthesis in simulated craters: intermediates, products and mechanism, *Frontiers in Astronomy and Space Sciences*, **2022**, *9*, 882145.

TẠP CHÍ KHOA HỌC
TRƯỜNG ĐẠI HỌC QUY NHƠN

Tổng quan về thiết kế dạng tổ ong trong pin nhiên liệu vi sinh

Đinh Kha Lil[1], Đái Huệ Ngân[2,3], Trần Văn Mẫn[2,3,*]

[1]Bộ môn Hóa học, Khoa Khoa học Tự nhiên, Trường Đại học Cần Thơ, Thành phố Cần Thơ, Việt Nam
[2]Bộ môn Hóa Lý, Khoa hóa học, Trường Đại học Khoa học Tự nhiên, Đại học Quốc gia Thành phố Hồ Chí Minh, Thành phố Hồ Chí Minh, Việt Nam
[3]Đại học Quốc gia Thành phố Hồ Chí Minh, Thành phố Hồ Chí Minh, Việt Nam

Ngày nhận bài:21/12/2021; Ngày nhận đăng: 12/04/2022

TÓM TẮT

Các nhiên liệu hóa thạch khai thác từ vỏ Trái đất khi cháy trong động cơ đốt trong, động cơ phản lực để tạo ra năng lượng phát thải khí carbonic cùng các khí thải độc hại khác nên tác động xấu tới môi trường và bầu khí quyển cần hạn chế và thay thế bằng năng lượng tái tạo. Việt Nam đặt mục tiêu phát thải carbon ròng bằng không vào năm 2050 và đang thực hiện chuyển đổi sang các năng lượng mặt trời, gió, sinh khối, sóng biển. Pin nhiên liệu vi sinh là một hệ điện hóa tạo ra dòng electron bằng cách sử dụng các hợp chất hữu cơ làm chất khử và oxy trong không khí làm chất oxy hóa. Trong hai thập kỷ qua, pin nhiên liệu vi sinh (Microbial Fuel Cell - MFC) đã thu hút các nhà khoa học và công nghệ vì khả năng chuyển đổi trực tiếp năng lượng hóa học từ các hợp chất hữu cơ khác nhau thành năng lượng điện. Vì vậy, MFC là một cách hứa hẹn khai thác năng lượng từ sinh khối. Trong bài tổng quan này, một số kết quả của các phương pháp tiền xử lý sinh khối theo hướng thu hoạch năng lượng bằng MFC và các vi sinh vật được sử dụng trong MFC nhiên liệu sinh khối đã được trình bày. Ngoài ra, cách tiếp cận và thiết kế để cải thiện hiệu suất của MFC sử dụng sinh khối trong tương lai cũng được nêu. Bài tổng quan đánh giá hiệu suất và khả năng ứng dụng của các dòng chảy trong MFC dạng tổ ong, đồng thời cũng đánh giá hiệu năng hoạt động, ưu điểm và nhược điểm tương ứng, và các ứng dụng tiềm năng trong tương lai của MFC với dòng tuần hoàn.

Từ khóa: *Sinh khối, vận tốc dòng chảy, pin nhiên liệu vi sinh, thiết kế tổ ong.*

[*]Tác giả liên hệ chính.
Email: tvman@hcmus.edu.vn

JOURNAL OF SCIENCE
QUY NHON UNIVERSITY

Honeycomb designs in microbial fuel cells - A review

Kha Lil Dinh[1], Hue Ngan Dai[2,3], Van Man Tran[2,3,*]

[1]Department of Chemistry, College of Natural Sciences, Can Tho University, Can Tho City, Vietnam
[2]Department of Physical Chemistry, Faculty of Chemistry, University of Science, Ho Chi Minh City, Vietnam
[3] Viet Nam National University Ho Chi Minh City, Ho Chi Minh City, Vietnam

Received: 21/12/2021; Accepted: 12/04/2022

ABSTRACT

Fossil fuels, the hydrocarbons within Earth's crust impact on the environment and atmosphere during burning in internal combustion engine, jet engine to produce energy have to be limited and all the countries have turned their attention to renewable energy. Vietnam will reach its net-zero carbon emission target by 2050 and call for fairness and justice in climate change issues. In order to realise this purpose, the country has to exploit more and more energy from renewable resources such as solar power, wind power and biomass. Microbial fuel cell is an electrochemical system that produces the electron current by using the organic compounds as reductant and oxygen in the air as oxidant. Over the past two decades, microbial fuel cells (MFC) have gained attention because they can directly convert chemical energy from various organic compounds into electrical energy. In MFC, biomass energy is directly harvested as electricity, the most exploitable and versatile form of energy. Therefore, MFC is a promising way to get the energy from biomass, adding a new dimension to the biomass energy industry. In this review, some results of the biomass pretreatment methods towards power harvesting by MFC and the microorganisms used in the biomass fuel MFC were summarized. In addition, strategies to improve the performance of MFC using biomass and future scenarios were highlighted. This review aims to evaluate the performance and applicability of flows in honeycomb MFC. It also assesses the respective performances, advantages and disadvantages, and potential future applications of MFCs with recirculation flow.

Keywords: *Biomass, flow velocity, microbial fuel cell, honeycomb design.*

1. INTRODUCTION

Water shortage is one of the severe global issues; according to climate change forecasts, this problem will be even more pressing in the future.[1] The increase in water demand has led to a rise in the amount of wastewater generated. At the same time, the need for renewable energy becomes immediate because of fossil fuels' rapid depletion and the growing concern about climate change. Many countries worldwide are looking for more reliable, sustainable and cleaner substitutes such as biomass to reduce the need for fossil fuels. To date, biomass can be converted into different energy products such as fuel, heat, gas, and electricity. Microbial fuel cell (MFC) is a power generation device that uses bacteria as biological catalysts in organic matter oxidation from wastewater through respiration, thereby generating electricity.[2] It has considerable potential for applications in

**Corresponding author.*
E-mail: tvman@hcmus.edu.vn

https://doi.org/10.52111/qnjs.2022.16302

wastewater treatment,[3] electrical equipment,[4] and biosensors.[5] Recently, reactor designs with a scale of several hundred liters have been developed.[6] Shifting this technology from the laboratory scale to the actual pilot scale will bring the technology closer to practical application.

Several researchers found that fluid motion impacts the energy efficiency of MFCs significantly. Increasing flow parameters such as flow rate and recirculation flow rate have been shown to enhance the power produced by the MFC.[7] Mass transport is also an essential factor in improving MFC power production due to the effects of flow regime,[8] mass-liquid transfer, biofilm formation, and the substrates.[9] Suppose the mass transfer between the substrate and the biofilm is low, some bacteria may detach from the biofilm as environmental conditions become unfavorable,[10] thereby increasing the biofilm damage, activation loss and mass transfer loss of the MFC.[11] Furthermore, most of the MFCs introduced into wastewater treatment plants have continuous flow and cyclic flow regimes,[12] which complicates the investigation of the mass transfer due to the regime caused by convection.

This paper reviews the MFC honeycomb design and analyzes the aspects of the design that affect MFC performance to focus the research direction for MFC design improvement.

2. MICROBIAL FUEL CELL

MFC is an energy-producing device with bacteria as biocatalysts, converting the energy in organic compounds into electricity. A simple MFC setup is shown in Figure 1, consisting of an anode in the anode chamber and a cathode in the cathode chamber, separated by a proton exchange membrane (PEM). MFC works on the principle that a biocatalyst oxidizes organic matter in the anode chamber, releasing protons and electrons in the process, also generating CO_2. The anode electrode captures electrons and transfers them to the cathode via the outer circuit along with the movement of protons from the anode to the cathode through the PEM. At the cathode, electrons combine with protons and oxygen to form water.[13] In MFC, the Gibbs free energy of the reaction is negative. Therefore, the MFC's electromotive force (EMF) will be positive, which indicates possible spontaneous generation from the reactions. For example, in case acetate is used as the substrate at the anode, oxygen is the electron donor at the cathode ($[CH_3COO^-]$ = $[HCO_3^-]$ = 10 mM; pH = 7; 298.15 K; p_{O_2} = 0.2 bar),[14] then the reaction in the battery will be:

Anodic reaction: $CH_3COO^- + 4H_2O \rightleftharpoons 2HCO_3^- + 9H^+ + 8e^-$ E^o = -0.289 V *vs.* SHE

Cathodic reaction: $2O_2 + 8H^+ + 8e^- \rightleftharpoons 4H_2O$ E^o = 0.805 V *vs.* SHE

Overall reaction: $CH_3COO^- + 2O_2 \rightleftharpoons 2HCO_3^- + H^+$ ΔG = -847.6 kJ/mol; EMF = 1.094 V

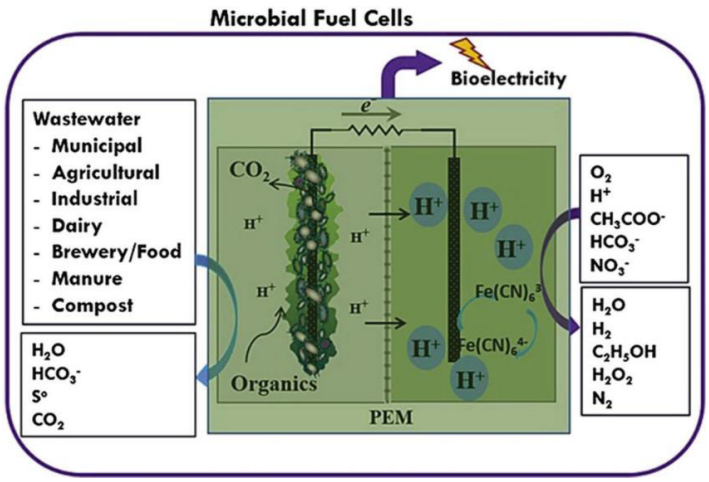

Figure 1. Structure diagram of microbial fuel cell.[15]

MFC technology has roused interest for more than 20 years not only because of the electric generation from wastes but because of its environmentally friendly wastewater treatment technology.[16] Many types of wastewater today contain many toxic wastes, which require expensive treatment before being discharged into the environment. Previous studies have demonstrated the ability of MFCs to treat wastes such as metal-derived wastewater, food, and urine and even produce drinking water after the treatment process.[17,18] MFC has coexisted with biological filter tanks in wastewater treatment to enhance pollution control and increase treatment capacity.[19] Most of the treatment methods aim to remove organic compounds that reduce chemical oxygen demand (COD), azo dyes,[20] and heavy metal waste.[21] The aeration system in wastewater treatment is reported to consume more than 54% of the electricity required in the treatment process. Since MFCs use anaerobic bacteria for the wastewater treatment process, this indicates potential energy saving in MFCs.[20] In addition, MFC-derived technologies such as MFC-based biosensors are expected to be one of its most promising applications. Having the capability to measure various parameters including bio-oxygen demand (BOD), chemical oxygen demad (COD), dissolved oxygen (DO), volatile fatty acids, toxic substances and microbial activity,[22] this device promises a reduction in time and cost in measuring the toxicity in water.

Recent advancement in the application of power generation capabilities includes the use of MFC to power a small computer (158 mW) directly and continuously without any management equipment and power source.[23]

The performance enhancement of the MFC was accomplished by using alternative electrode materials, different electrode surfaces, electroactive bacteria (EAB), substrate, and load resistance. The electrode material has a significant influence on the performance of the MFC.[24] Carbon materials are used as electrodes in MFC because they are non-corrosive, highly biocompatible, and exhibit some distinctive surface characteristics of electrode materials. Modification of the electrode material has been shown to be an effective way to improve the performance of the MFC.[25] This change in the physical and chemical properties of the electrode helps the microorganism bind and transfer electrons better. The efficiency of MFC can be increased by improving bacterial adhesion and electron transfer along with the modification of the electrode surface.[26]

The biofilm attached to the electrode is a crucial element of electrochemical bioreaction.[27] The growth and development of biofilms on the MFC electrodes, especially on the anode electrode, will help carry out the oxidation of organic matter and transfer electrons to the cathode.[28] The anode electrode of the MFC must contain a stable and homogeneous bioreactor for enhanced energy generation.[29] Biofilm cultures are often contaminated by wastewater or the entry of other competing microbial species, which can reduce performance. Next, the performance of MFC is highly dependent on the nature of the substrate. Substances can be classified into simple molecular structures such as the commonly sed glucose and acetates and more complex structures such as molasses and cellulose.[17] From a chemical characterization perspective, the nature of the substrate used by the bacteria during aerobic or anaerobic respiration will affect the electron donation rate in the MFC. This influence is based on the complexity of the different bacterial species used in the MFCs.[30]

In summary, the electrode properties and the correlation between electrode, substrate, and bacteria are the main factors affecting the performance of MFC. It can be seen that the development of MFC technology is a diverse combination of specialties such as biochemistry, electrochemistry, mechanical engineering, and materials science. Alot of work are doing in order to improve the preformance of MFC such as *(i)* the Nafion membrane[31] *(ii)* pre- treatment of biomass as bamboo,[32,33] *(iii)* hydrogen revolution directly form fermentation of biomass[34] and *(iv)* power generation with higher eficiency.[35,36]

https://doi.org/10.52111/qnjs.2022.16302

3. HONEYCOMB DESIGN

3.1. Structure of honeycomb MFC

The honeycomb straight-line press is a device widely used in dynamic research works and has many practical applications. They have a metal or ceramic tubular structure aligned parallel to the flow direction and have the shape of a honeycomb.[37] These structures are used to achieve different goals, such as generating shear forces with uniform geometry. They are used in wind tunnels to reduce velocities caused by the eddy motion of the air stream during entry. They are also applied in flat plate solar collectors to reduce and prevent heat loss and enhance the natural thermal convection process.[38] The application of honeycomb structure in MFCs is relatively new. To the authors' knowledge, this design was developed only by Wang et al. The honeycomb MFC design is shown in Figure 2, consisting of an anode and a cathode chamber separated from each other by a proton exchange membrane. The anode chamber has a symmetrical structure, including two booster tanks and two honeycomb structures. It is connected to a pump system to facilitate continuous flow of the liquid in the chamber.

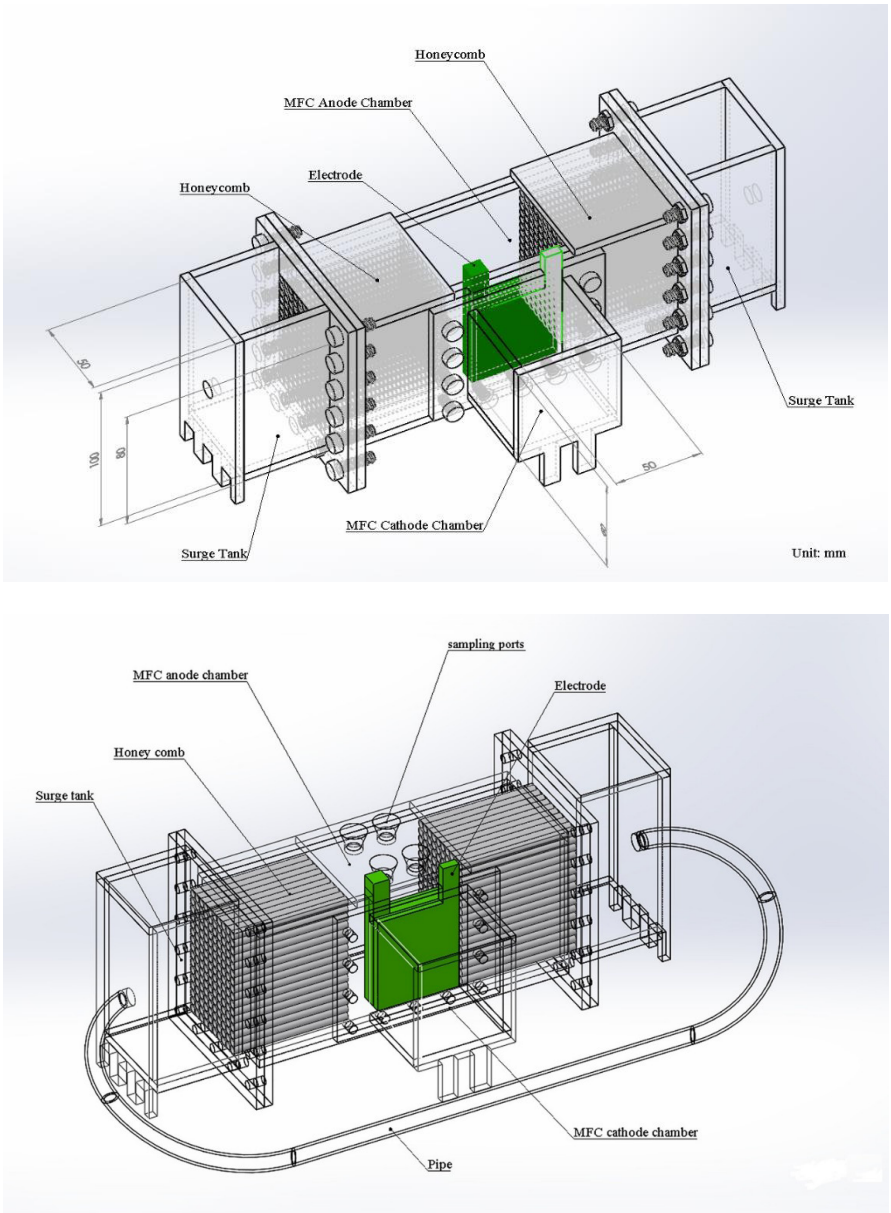

Figure 2. Perspective of two-chamber honeycomb MFC.[36]

MFC technology can be applied in wastewater treatment plants with a recirculating flow mode. The cyclical flow whill promote a mass transfer that depends not only on diffusion but also on the motion of the anode liquid.

In fluid mechanics, the Reynolds number (R_e) is a dimensionless quantity representing the relative magnitude of the influence caused by inertia and viscosity on flow resistance.[39]

$$R_e = \frac{\rho V D_T}{\mu}$$

Where: ρ is the density of the liquid (kg/m^3), V is the flow rate (m/s), D_T is the hydraulic diameter (m), and μ is the viscosity of the liquid (kg/ms). Reynolds number includes basic properties of liquids and physical quantities such as flow velocity, fluid density, and viscosity.[40] Therefore, this parameter describes the hydrodynamic effect on the power production of the MFC.

3.2. Impact of hydrodynamic boundary layer

The effect of the hydrodynamic boundary layer is a determinant of performance in a cyclic MFC reactor. The flux parameters are essential because the main component of wastewater is H_2O. Its motion has an outstanding feature in MFC performance and biological properties.[41] There are several methods used to maintain thin hydrodynamic boundary layer thickness, such as by placing the electrode near the flow inlet,[42] using thin porous electrode,[43] using flow controls to prevent the development of hydrodynamic boundary layers.[44] The working mechanism model of the hydrodynamic boundary layer effect is illustrated in Figure 3.

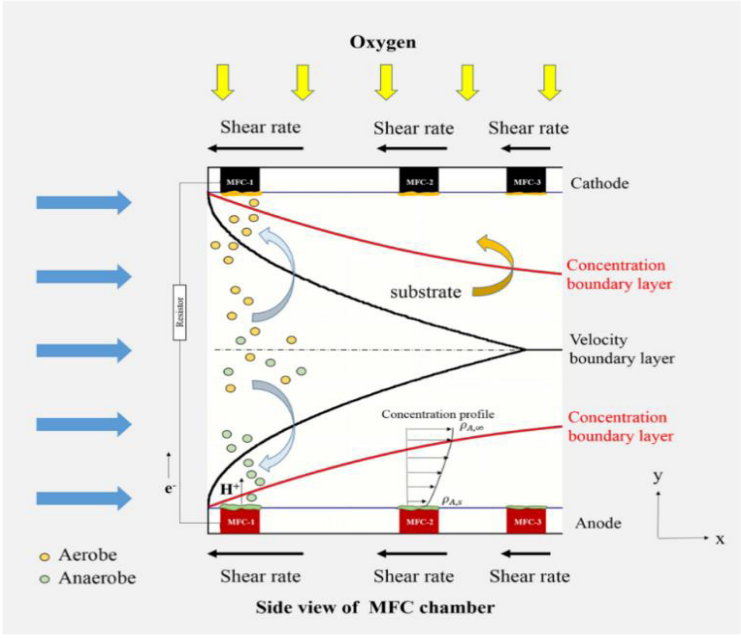

Figure 3. Diagram of boundary layers in a microbial fuel cell chamber.[45]

Figure 3 shows that the thickness of the hydrodynamic boundary layer will increase as the distance from the leading edges of the chamber wall increases. The flow velocity gradient will cause strong shear stress in the hydrodynamic boundary layer.[44] Therefore, the influence of the hydrodynamic boundary layer will affect not only the biofilm structure but also the mass transfer of the substrate.[46]

Chen *et al.*[45] tested honeycomb MFCs with various electrode distances from the chamber wall (at 1, 6, and 9 cm) to see the effect on the hydrodynamic boundary layer. It is reported that reducing the hydrodynamic boundary layer thickness on the electrode can significantly enhance biofilm formation and substrate mass transfer.

https://doi.org/10.52111/qnjs.2022.16302

Biofilms tend to increase their cohesion to adapt to the flow environment.[47] Li *et al.*[48] showed that the gravity effect applied to the MFC facilitated the bacterial attachment to the electrode and thickened the biofilm.

3.3. Effect of flow rate

Ieropoulos *et al.*[49] reported that the MFC performance improved when the flow rate was increased. The velocity and direction of flow can significantly affect the mass transfer of particles in the anodic solution. As mentioned, MFC current generation was directly related to the biofilm on the electrodes. The growth of thicker biofilms facilitated electron transfer to the cathode, thereby improving reactor efficiency.[50] The optimal rate in the MFC will enhance microbial activity and increase the electron transfer rate in biological media, which will reduce the activation of polarization. Meanwhile, turbulence will have the opposite effects. Wang *et al.*[51] reported that the energy density in the honeycomb MFC increased as the flow rate increased from 0 to 40 mL/min. However, as the rate increased to 240 mL/min, the power density decreased. This decrease was explained as a result of biofilm leaching at the anode. In addition, increasing the flow rate can cause oxygen permeation through the PEM from the cathode to the anode chamber. This will increase the presence of oxygen in the anode chamber which will inhibit EAB growth.

Ketep *et al.*[53] reported that the favorable environment for the growth and development of EAB was pH neutral. Under alkaline or acidic conditions, the activity of EAB in the MFC will be disrupted. It was found that the anode pH value between 7.0 and 7.55 is suitable for the operation of EAB.[54] The slow transfer of protons to the cathode compared with proton generation due to EAB activity can lead to decreased EAB activity due to their unfavorable acidic environment.[55] Maintaining the flow rate resulted in the MFC‘s ability for stability in pH.[51] Conventional methods use buffer solutions to slow acidification and maintain pH close to neutral.[56] Although using buffer solutions in an MFC system has many advantages, there is still a long way to go to scale the application because it is quite expensive. Another approach is to enhance proton transfer to stabilize pH at the anode. Cyclic mode honeycomb MFC is a promising strategy for improving proton transfer capacity, thereby improving power generation efficiency and solving the problem of using buffer solutions to stabilize the pH at low temperatures at the anode chamber.

Therefore, it can be asserted that the average velocity can be beneficial to the reactor performance due to the homogeneity of the ions in the reactor. This can lead to a large mass transfer of ions and particles to microorganisms on the biofilm and eventually to the growth and attachment of thick biofilms on the anode.

3.4. Effect of channel diameter and pipe diameter

Channel and pipe diameters are important factors in hydrodynamics. Kaji and Azzopardi[57] reported that as the pipe diameter increased, the velocity gradient decreased. The flow geometry also affects the flow velocity of the liquid in the anode. This is also demonstrated in some publications,[58,59] who affirmed that the flow velocity increases as the pipe diameter decreases. Small diameter pipes have greater resistance near the inlet. They have a circular waveform near the outlet, which is the leading cause of their chaotic pattern.

Sangeetha *et al.*[41] reported that the honeycomb channel diameter affects the removal of organic matter in the anode chamber of the honeycomb MFC. They also demonstrated that the honeycomb channel diameter affects the anode bio-thickness. Honeycomb structures with optimized channel diameters can support efficient energy and mass transfer inside the reactor.

3.5. Effect of distance between two electrodes

With respect to the influence of the anode electrode position in honeycomb MFC, Wang

et al.[60] reported that the anode-to-film distance with a value of x = 0.0 cm gives the best performance in honeycomb MFC. This could be because proton movement is restricted to the cases where the anode electrode is located far from the PEM. In addition, Xu *et al.*[61] also pointed out that the conductivity is affected by the biological fouling phenomenon that occurs on the surface of PEM when the PEM is in direct contact with the liquid in the anode.

Table 1. Studies using recirculating honeycomb reactors

Flow rate (mL/min)	Reynolds number	Electrode spacing (cm)	Flow channel diameter (cm)	OCP** (V)	Maximum power density (mW/m^2)	References
0	0	NA	1.0	0.45	2.19	[46]
4	0.37	NA	1.0	0.67	2.93	[46]
40	3.7	NA	1.0	0.77	4.5	[46]
240	44.8	NA	1.0	0.27	2.77	[46]
0	0.0	5.0	NA	≅ 0.7	1512.4	[57]
0.06	0.016	5.0	NA	≅ 0.7	1705.7	[57]
0.58	0.16	5.0	NA	≅ 0.7	1922.3	[57]
5.83	1,6	5.0	NA	≅ 0.7	2383.5	[57]
58.3	16	5.0	NA	≅ 0.7	2422.8	[57]
58.0	16	0.0	0.7	0.62	361.8	[55]
58.0	16	3.0	0.7	0.65	130.8	[55]
58.0	16	6.0	0.7	0.68	308.6	[55]
58.0	16	0.0	0,4	0.51	333.0	
58.0	16	0.0	0,7	0.69	430.0	[36]
58.0	16	0.0	1.0	0.19	137. 0	[36]

**OCP – Open Ciruit Potential

4. CONCLUSIONS

The MFC system has a bright future not only because of using the cheaper material but also of combining techniques for generating electric power and treating wastewater. An overview of the new honeycomb MFC design has been presented and elucidated. The influence of flow and related design factors are presented in Table 1. In order to systematize optimal design conditions, the optimal reactor speed was determined at 40 mL/min. The reactors achieved maximum voltage output, power, and current density with reduced internal resistance. When the flow rate is too large, biofilm washout will occur, resulting in reduced efficiency. The effect of hydrodynamic boundary layer in recirculation MFC is a vital factor influencing mass transfer and biofilm formation. Electrode placement selection and flow control are two effective and economical methods of maintaining the hydrodynamic boundary layer thickness. The honeycomb tube diameter of 0.7 cm is optimal for enhanced COD removal and power generation efficiency. The electrode distance affects the transport of protons from the anode to the cathode.

Currently, the problems of material cost and unclear surface modification mechanisms hinder the practical application of MFC. The honeycomb design has great significance in

https://doi.org/10.52111/qnjs.2022.16302

reducing operating costs, improving efficiency, and contributing to the operation of an MFC system with recirculating flow.

REFERENCES

1. N. Mancosu, R. L. Snyder, G. Kyriakakis, D. Spano. Water scarcity and future challenges for food production, *Water*, **2015**, *7*(3), 975-992.
2. K. Obileke, H. Onyeaka, E. L. Meyer, N. Nwokolo. Microbial fuel cells, a renewable energy technology for bio-electricity generation: a mini-review, *Electrochemistry Communications*, **2021**, 107003.
3. W.-f. Liu, S.-a. Cheng. Microbial fuel cells for energy production from wastewaters: the way toward practical application, *Journal of Zhejiang University Science A*, **2014**, *15*(11), 841-861.
4. D. G. Arboleda Avilés, O. F. Núñez Barrionuevo, O. F. Sánchez Olmedo, B. D. Chinchín Piñan, D. A. Arboleda Briones, R. A. Bahamonde Soria. Application of a direct current circuit to pick up and to store bioelectricity produced by microbial fuel cells, *Revista Colombiana de Química*, **2019**, *48*(3), 26-35.
5. J. Z. Sun, G. Peter Kingori, R. - W. Si, D. - D. Zhai, Z. - H. Liao, D.-Z. Sun, T. Zheng, Y. - C. Yong. Microbial fuel cell-based biosensors for environmental monitoring: a review, *Water Science and Technology*, **2015**, *71*(6), 801-809.
6. H. Hiegemann, T. Littfinski, S. Krimmler, M. Lübken, D. Klein, K. - G. Schmelz, K. Ooms, D. Pant, M. Wichern. Performance and inorganic fouling of a submergible 255 L prototype microbial fuel cell module during continuous long-term operation with real municipal wastewater under practical conditions, *Bioresource Technology*, **2019**, *294*, 122227.
7. C. Munoz-Cupa, Y. Hu, C. C. Xu, A. Bassi. An overview of microbial fuel cell usage in wastewater treatment, resource recovery and energy production, S*cience of the Total Environment*, **2020**, 142429.
8. S. Pinck, L. M. Ostormujof, S. Teychené, B. Erable. Microfluidic microbial bioelectrochemical systems: an integrated investigation platform for a more fundamental understanding of electroactive bacterial biofilms, *Microorganisms*, **2020**, *8*(11), 1841.
9. D. Taherzadeh, C. Picioreanu, H. Horn. Mass transfer enhancement in moving biofilm structures, *Biophysical Journal*, **2012**, *102*(7), 1483-1492.
10. J. B. Kaplan. Biofilm dispersal: mechanisms, clinical implications, and potential therapeutic uses, *Journal of Dental Research*, **2010**, *89*(3), 205-218.
11. M. Rahimnejad, G. Najafpour, A. A. Ghoreyshi. Effect of mass transfer on performance of microbial fuel cell, *Intech*, **2011**, *5*, 233-250.
12. Y. Wang, Y. Zhao, L. Xu, W. Wang, L. Doherty, C. Tang, B. Ren, J. Zhao. Constructed wetland integrated microbial fuel cell system: looking back, moving forward, *Water Science and Technology*, **2017**, *76*(2), 471-477.
13. Z. Du, H. Li, T. Gu. A state of the art review on microbial fuel cells: a promising technology for wastewater treatment and bioenergy, *Biotechnology Advances*, **2007**, *25*(5), 464-482.
14. R. A. Rozendal, H. V. Hamelers, K. Rabaey, J. Keller, C. J. Buisman. Towards practical implementation of bioelectrochemical wastewater treatment, *Trends in Biotechnology*, **2008**, *26*(8), 450-459.
15. V. G. Gude. Wastewater treatment in microbial fuel cells–an overview, *Journal of Cleaner Production*, **2016**, *122*, 287-307.
16. M. Schechter, A. Schechter, S. Rozenfeld, E. Efrat, R. Cahan. Anode biofilm, *Technology and Application of Microbial Fuel Cells*, **2014**, 57.
17. D. Pant, G. Van Bogaert, L. Diels, K. Vanbroekhoven. A review of the substrates used in microbial fuel cells (MFCs) for sustainable energy production, *Bioresource Technology*, **2010**, *101*(6), 1533-1543.
18. T. Catal, A. Kul, V. E. Atalay, H. Bermek, S. Ozilhan, N. Tarhan. Efficacy of microbial fuel cells for sensing of cocaine metabolites in urine-based wastewater, *Journal of Power Sources*, **2019**, *414*, 1-7.

19. A. J. Mohammed, Z. Z. Ismail. Slaughterhouse wastewater biotreatment associated with bioelectricity generation and nitrogen recovery in hybrid system of microbial fuel cell with aerobic and anoxic bioreactors, *Ecological Engineering*, **2018**, *125*, 119-130.

20. A. G. Capodaglio, G. Olsson. Energy issues in sustainable urban wastewater management: use, demand reduction and recovery in the urban water cycle, *Sustainability*, **2020**, *12*(1), 266.

21. A. S. Mathuriya, J. Yakhmi. Microbial fuel cells to recover heavy metals, *Environmental Chemistry Letters*, **2014**, *12*(4), 483-494.

22. Y. Cui, B. Lai, X. Tang. Microbial fuel cell-based biosensors, *Biosensors*, **2019**, *9*(3), 92.

23. X. A. Walter, J. Greenman, I. A. Ieropoulos. Microbial fuel cells directly powering a microcomputer, *Journal of Power Sources*, **2020**, *446*, 227328.

24. S. Kalathil, S. Patil, D. Pant. *Microbial fuel cells: electrode materials*, Elsevier, Amsterdam, The Netherlands, 2017, 1-10.

25. M. Zhou, M. Chi, J. Luo, H. He, T. Jin. An overview of electrode materials in microbial fuel cells, *Journal of Power Sources*, **2011**, *196*(10), 4427-4435.

26. P. Choudhury, U. S. Prasad Uday, T. K. Bandyopadhyay, R. N. Ray, B. Bhunia. Performance improvement of microbial fuel cell (MFC) using suitable electrode and Bioengineered organisms: a review, *Bioengineered*, **2017**, *8*(5), 471-487.

27. M. N. Gatti, R.H. Milocco. A biofilm model of microbial fuel cells for engineering applications, *International Journal of Energy and Environmental Engineering*, **2017**, *8*(4), 303-315.

28. T. - H. Lan, C. - T. Wang, T. Sangeetha, Y. - C. Yang, A. Garg. Constructed mathematical model for nanowire electron transfer in microbial fuel cells, *Journal of Power Sources*, **2018**, 402, 483-488.

29. L. Wang, C. Yang, T. Sangeetha, Z. He, Z. Guo, G. Lei, A. Wang, W. Liu. Methane production in a bioelectrochemistry integrated anaerobic reactor with layered nickel foam electrodes, *Bioresource Technology*, **2020**, 123657.

30. C. Santoro, C. Arbizzani, B. Erable, I. Ieropoulos. Microbial fuel cells: from fundamentals to applications. A review, *Journal of Power Sources*, **2017**, *356*, 225-244.

31. H. H. Lam, D. T. Tran, T. T. H. Dinh, E. Korneeva, V. T. Nguyen, K. Yoshimura, S. Hasegawa, S. Sawada, M. V. Tran, Q. H. Nguyen, A. T. Luu, V. P. Dinh, Q. L. Le, Y. Maekawa. Morphological characterization of grafted polymer electrolyte membranes at a surface layer for fuel cell application, *Journal of Applied Polymer Science,* **2021***, 139*(14), 51910.

32. H. N. Dai, T. K. N Le, T. K. T. Huynh, T. A. D. Nguyen, M. V. Tran. Thermo-pretreatment on bamboo biomass with ammonia, *Journal of Science and Technology*, **2016**, *54*(4B), 24-29.

33. H. N. Dai, T. K. T. Huynh, T. A. D. Nguyen, T. V. V. Do, M. V. Tran. Hydrothermal and steam explosion pretreatment of bambusa stenostachya bamboo, *Waste and Biomass Valorization*, **2021**, *12*(9), 1-10.

34. H. N. Dai, T. T. Vo, T. A. D. Nguyen, M. V. Tran, L. P. M. Le. Hydrogen production from acidic, alkaline and steam exploded bambusa stenostachya hydrolysates in dark fermentation, *Biomass Conversion and Biorefinery*, **2021**.

35. H. N. Dai, T. A. D. Nguyen, L. P. M. Le, M. V. Tran, T. - H. Lan, C. - T. Wang. Power generation of Shewanella oneidensis MR-1 microbial fuel cells in bamboo fermentation effluent, *International Journal of Hydrogen Energy*, **2020**, *46*(31), 16612-16621.

36. K. L. Dinh, C. T. Wang, H. N. Dai, V. M. Tran, M. L. P. Le, I. A. Saladaga, Y. A. Lin. Lactate and acetate applied in dual-chamber microbial fuel cells with domestic wastewater, *International Journal of Energy Research*, **2021**, *45(7)*, 10655-10666.

37. T. Sangeetha, I. - T. Li, T. - H. Lan, C. - T. Wang, W. - M. Yan. A fluid dynamics perspective on the flow dependent performance of honey comb microbial fuel cells, *Energy*, **2021**, *214*, 118928.

https://doi.org/10.52111/qnjs.2022.16302

38. P. R. Satpathy, R. Sharma, S. Jena, A. shade dispersion interconnection scheme for partially shaded modules in a solar PV array network, *Energy*, **2017**, *139*, 350-365.

39. M. V. Dyke. *An album of fluid motion*, USA, 1982.

40. J. Welty, G. L. Rorrer, D. G. Foster. *Fundamentals of momentum, heat, and mass transfer*, John Wiley & Sons, 2020.

41. T. Sangeetha, I. - T. Li, T. - H. Lan, C. - T. Wang, W.-M. Yan. A fluid dynamics perspective on the flow dependent performance of honey comb microbial fuel cells, *Energy*, **2021**, *214*, 118928.

42. D. Ye, Y. Yang, J. Li, X. Zhu, Q. Liao, B. Deng, R. Chen. Performance of a microfluidic microbial fuel cell based on graphite electrodes, *International Journal of Hydrogen Energy*, **2013**, *38*(35), 15710-15715.

43. T. H. Sleutels, H. V. Hamelers, C. J. Buisman. Effect of mass and charge transport speed and direction in porous anodes on microbial electrolysis cell performance, *Bioresource technology*, **2011**, *102*(1), 399-403.

44. Y. Yang, D. Ye, Q. Liao, P. Zhang, X. Zhu, J. Li, Q. Fu. Enhanced biofilm distribution and cell performance of microfluidic microbial fuel cells with multiple anolyte inlets, *Biosensors and Bioelectronics*, **2016**, *79*, 406-410.

45. Y. - M. Chen, C. - T. Wang, Y. - C. Yang. Effect of wall boundary layer thickness on power performance of a recirculation microbial fuel cell, *Energies*, **2018**, *11*(4), 1003.

46. A. Ter Heijne, O. Schaetzle, S. Gimenez, F. Fabregat-Santiago, J. Bisquert, D. P. Strik, F. Barriere, C. J. Buisman, H. V. Hamelers. Identifying charge and mass transfer resistances of an oxygen reducing biocathode, *Energy & Environmental Science*, **2011**, *4*(12), 5035-5043.

47. H. Beyenal, Z. Lewandowski. Internal and external mass transfer in biofilms grown at various flow velocities, *Biotechnology progress*, **2002**, *18*(1), 55-61.

48. T. Li, L. Zhou, Y. Qian, L. Wan, Q. Du, N. Li, X. Wang. Gravity settling of planktonic bacteria to anodes enhances current production of microbial fuel cells, *Applied energy*, **2017**, *198*, 261-266.

49. I. Ieropoulos, J. Winfield, J. Greenman. Effects of flow-rate, inoculum and time on the internal resistance of microbial fuel cells, *Bioresource Technology*, **2010**, *101*(10), 3520-3525.

50. N. Eaktasang, C. S. Kang, S. J. Ryu, Y. Suma, H. S. Kim. Enhanced current production by electroactive biofilm of sulfate-reducing bacteria in the microbial fuel cell, *Environmental Engineering Research,* **2013***, 18*(4), 277-281.

51. C. - T. Wang, Y. - S. Huang, T. Sangeetha, W. - M. Yan. Assessment of recirculation batch mode operation in bufferless bio-cathode microbial Fuel Cells (MFCs), *Applied Energy*, **2018**, *209*, 120-126.

52. L. Zhang, X. Zhu, H. Kashima, J. Li, D. - d. Ye, Q. Liao, J. M. Regan. Anolyte recirculation effects in buffered and unbuffered single-chamber air-cathode microbial fuel cells, *Bioresource Technology*, **2015**, *179*, 26-34.

53. S. F. Ketep, A. Bergel, M. Bertrand, W. Achouak, E. Fourest. Lowering the applied potential during successive scratching/re-inoculation improves the performance of microbial anodes for microbial fuel cells, *Bioresource Technology*, **2013**, *127*, 448-455.

54. V. R. Nimje, C. Y. Chen, C. C. Chen, J. Y. Tsai, H. - R. Chen, Y. M. Huang, J. - S. Jean, Y. - F. Chang, R. - C. Shih. Microbial fuel cell of Enterobacter cloacae: Effect of anodic pH microenvironment on current, power density, internal resistance and electrochemical losses, *International Journal of Hydrogen Energy*, **2011**, *36*(17), 11093-11101.

55. G. Jadhav, M. Ghangrekar. Performance of microbial fuel cell subjected to variation in pH, temperature, external load and substrate concentration, *Bioresource Technology*, **2009**, *100*(2), 717-723.

56. G. C. Gil, I. S. Chang, B. H. Kim, M. Kim, J. - K. Jang, H. S. Park, H. J. Kim. Operational parameters affecting the performance of a mediator-less microbial fuel cell, *Biosensors and Bioelectronics*, **2003**, *18*(4), 327-334.

57. R. Kaji, B. Azzopardi, The effect of pipe diameter on the structure of gas/liquid flow in vertical pipes, *International Journal of Multiphase Flow*, **2010**, *36*(4), 303-313.

58. M. Vijayan, S. Jayanti, A. Balakrishnan, Effect of tube diameter on flooding, *International Journal of Multiphase Flow*, **2001**, *27(5)*, 797-816.

59. X. Li, L. Hu, F. Shang. Flame downwash transition and its maximum length with increasing fuel supply of non-premixed jet in cross flow, *Energy*, **2018**, *164*, 298-305.

60. C. T. Wang, I. T. Li, J. H. Jang. Effect of electrode spacing on the performance of microbial fuel cells with a honeycomb flow straightener, *International Journal of Energy Research*, **2020**, *44*(14), 12136-12144.

61. J. Xu, G. P. Sheng, H. - W. Luo, W. - W. Li, L. - F. Wang, H. - Q. Yu. Fouling of proton exchange membrane (PEM) deteriorates the performance of microbial fuel cell, *Water Research*, **2012**, *46*(6), 1817-1824.

https://doi.org/10.52111/qnjs.2022.16302

TẠP CHÍ KHOA HỌC
TRƯỜNG ĐẠI HỌC QUY NHƠN

Về một điều kiện thác triển liên tục nghiệm phương trình vi phân ngẫu nhiên trong không gian Hilbert

Mai Thành Tấn*

Khoa Toán và Thống kê, Trường Đại học Quy Nhơn, Việt Nam

Ngày nhận bài: 09/11/2021; Ngày nhận đăng: 15/12/2021

TÓM TẮT

Bài báo tập trung nghiên cứu khái niệm về nghiệm yếu và nghiệm tích phân (mild solutions) của phương trình vi phân ngẫu nhiên phi tuyến trên không gian Hilbert với hệ các toán tử phụ thuộc thời gian, không bị chặn. Chúng tôi đưa ra một điều kiện để hai khái niệm nghiệm tích phân và nghiệm yếu ở trên là trùng nhau và đồng thời nghiên cứu thác triển liên tục nghiệm tích phân trên các không gian Hilbert. Dạng phương trình và các khái niệm về nghiệm chúng tôi nghiên cứu bắt nguồn trong lĩnh vực toán công nghiệp.

Từ khóa: *Nghiệm yếu phương trình vi phân ngẫu nhiên, hệ tiến hoá không thuần nhất phụ thuộc thời gian, nghiệm giải tích yếu.*

* *Tác giả liên hệ chính.*
Email: maithanhtan@qnu.edu.vn

https://doi.org/10.52111/qnjs.2022.16303

JOURNAL OF SCIENCE
QUY NHON UNIVERSITY

A note on continuously extended solutions of stochastic differential equations on Hilbert spaces

Mai Thanh Tan*

Faculty of Mathematics and Statistics, Quy Nhon University, Vietnam

Received: 09/11/2021; Accepted: 15/12/2021

ABSTRACT

We study about mild solutions and weak solutions of non-linear stochastic differential equations (SDEs) in Hilbert spaces for the case of family of time-dependent and unbounded operators and get some conditions that weak solutions to become mild solutions and vice versa. We also study continuously extension of mild solutions on Hilbert spaces. Our equation and concept of solutions are arisen as a stochastic partial differential equation (SPDE) in industrial mathematics.

Keywords: *Weak solution of SDE, non-time homogeneous evolution systems, analytically weak solutions.*

1. INTRODUCTION

Let us denote by $(\Omega, \mathcal{F}, \mathbb{P})$ a probability space where the family $\mathcal{F}$ of subsets of Ω is a σ-algebra, and $\mathbb{P}$ is a probability measure on $(\Omega, \mathcal{F})$. It is always assumed that G, H are separable Hilbert spaces; the Q-Wiener process $W = (W(t))_{t\in[0,T]}, 0 < T < \infty$, is defined on $(\Omega, \mathcal{F}, \mathbb{P})$ together with a normal filtration $(\mathcal{F}_t)_{t\geq 0}$ and is valued in G. Consider the following stochastic differential equation

$$\begin{aligned} dX(t) &= \big(L(t)X(t) + F(t)\big)dt + AdW(t), \\ X(t_0) &= \xi, \quad 0 \leq t_0 \leq t \leq T, \end{aligned} \tag{1}$$

where for all $t \in [0, T]$ the linear operator $L(t) : D(L(t)) \subset H \longrightarrow H$ is closed and densely defined on H; the operator $A : G \longrightarrow H$ is linear and continuous, F is an H-valued process, pathwise Bochner integrable on $[0, T]$, and the initial value ξ is an $\mathcal{F}_{t_0}$-measurable random variable getting values in H.

There are many mathematician studying on the equation (1). DaPrato and Zabczyk[1] studied the case operators are independent in time. Instead of separable Hilbert sapces, Manthey and Zausinger, see,[2] constructed mild solutions to (1) in weighted L^p spaces. In,[3] Prevot and Roeckner considered for $L(t)$ coercive variational solutions to (1). Veraar and Zimmerschied[4] considered the case of the family $L(t)$ is uniformly sectorial in $[t_0, T]$. Baur, Grothaus, and Mai, see,[5] give some conditions for existence and uniqueness of analytically weak solution to (1) and apply these results to linearized versions of a non-linear stochastic partial differential algebraic equation arising in industrial mathematics, that leads to the time-dependent case with the state space is some Sobolev space.

**Corresponding author.*
Email: maithanhtan@qnu.edu.vn

https://doi.org/10.52111/qnjs.2022.16303

In this paper, we continue to study on solutions in[5] and give some conditions that weak solutions become mild solutions and vice versa and study continuously extended (mild) solutions on some Hilbert spaces.

2. PRELIMINARIES

From now on, we always assume that $(G, \langle\cdot,\cdot\rangle_G)$ and $(H, \langle\cdot,\cdot\rangle_H)$ are separable Hilbert spaces and $\|\cdot\|_G := \sqrt{\langle\cdot,\cdot\rangle_G}$ and $\|\cdot\|_H := \sqrt{\langle\cdot,\cdot\rangle_H}$ are the corresponding norms generated by the inner products, and $0 < T < \infty$. Let $(L(G,H), \|\cdot\|_{L(G,H)})$ be the space of all bounded linear operators from G to H together with the operator norm $\|\cdot\|_{L(G,H)}$; and $L(H) := L(H,H)$. Assume that the linear operator $L : D(L) \subset G \longrightarrow H$ is densely defined on G. We also denote $(L^*, D(L^*))$ the Hilbert adjoint operator of unbounded operator $(L, D(L))$ for the case $G \equiv H$, see.[6] In the application, we shall use concepts e.g. *stable family of operators, part of an operator in some subspace, invariant and admissible subspaces* as in.[7]-[9] The measurability of $L(G,H)$-valued functions will be considered as in.[1]

Definition 2.1. Let H be a Banach space and $L(H)$ be the space of linear bounded operators in H. A family $(S(t))_{t\geq 0} \subset L(H)$ is called a semi-group on H if

(i) $S(0) = Id$;

(ii) $S(t+r) = S(t)S(r)$ for all $t, r \geq 0$.

One concerns about a property of the family $(S(t))_{t\geq 0}$ at the "origin" $t = 0$ that $S(t)$ "converges" to Id as t decreases to 0. If the convergence is in the uniform topology on $L(H)$, i.e., $\lim_{t\downarrow 0} \|S(t) - Id\|_{L(H)} = 0$, then the family $(S(t))_{t\geq 0}$ is called a uniformly continuous semi-group. If it happens with the strong topology on $L(H)$, i.e. for all $u \in H$, $\lim_{t\downarrow 0} \|S(t)u - u\|_H = 0$, then $(S(t))_{t\geq 0}$ is called a *strongly continuous semi-group*; or is called shortly as a "semi-group of class C_0" or "C_0-semi-group". Of course, uniformly continuous semi-groups are also C_0-semi-groups.

Definition 2.2. A map $\Phi : \Omega \longrightarrow L(G,H)$ is called *strongly measurable* if for arbitrary $v \in G$ the function $\Phi v : (\Omega, \mathcal{F}) \longrightarrow (H, \mathcal{B}(H))$ is measurable. And $\Phi : \Omega \longrightarrow L(G,H)$ is said to be *Bochner integrable* if for all $v \in G$, the (H-valued) function Φv is Bochner integrable and there exists a linear bounded operator $\Psi \in L(G,H)$ such that

$$\int_\Omega \Phi(\omega)v\mathbb{P}(d\omega) = \Psi v, \ v \in G.$$

The operator Ψ is called the Bochner integral of Φ and is denoted by $\int_\Omega \Phi(\omega)\mathbb{P}(d\omega)$ or $\int_\Omega \Phi d\mathbb{P}$.

3. CONTINUOUSLY EXTENDED SOLUTIONS OF SPDEs

In this section, we continue to study the concepts mild and weak solutions as in[5] for nonlinear equations and will give conditions that weak solutions become mild solutions and vice versa. Moreover, we also study continuously extended mild solutions on Hilbert spaces.

We consider again the following equation on a separable Hilbert space H

$$\begin{cases} dX(t) = \big(L_0X(t) + L_1(t)X(t) + F(t, X(t))\big)dt + \\ \qquad\qquad +A(t, X(t))dW(t), \quad \tau \leq t \leq T \\ X(\tau) = \xi \in H, \end{cases} \tag{2}$$

where $W := (W(t))_{t\geq\tau}$ is an H-valued Q-Wiener process on a probability space $(\Omega, \mathcal{F}, \mathbb{P})$ together with a normal filtration $(\mathcal{F}_t)_{t\geq\tau}$.

Assumption 3.1. We assume that

(i) $(L_0, D(L_0))$ is the generator of a C_0-semi-group $(S(t))_{t\geq 0}$ on a Hilbert space H,

(ii) $L_1(t) \in L(H), \ \forall\, t \in [\tau, T]$,

https://doi.org/10.52111/qnjs.2022.16303

(iii) The function $F : [0,T] \times \Omega \times H \longrightarrow H$ is a measurable function on measurable spaces $(\Omega_T \times H, \mathscr{P}_T \times \mathcal{B}(H))$ and $(H, \mathcal{B}(H))$.

(iv) The function $A : [0,T] \times \Omega \times H \longrightarrow L_2^0$ is measurable on spaces $(\Omega_T \times H, \mathscr{P}_T \times \mathcal{B}(H))$ and $(L_2^0, \mathcal{B}(L_2^0))$, respectively.

(v) There exists a positive constant C such that $\forall u, u_1, u_2 \in H, t \in [0,T]$, and $\forall \omega \in \Omega$ we have

$$\|F(t,\omega;u_1) - F(t,\omega;u_2)\| + \\ + \|A(t,\omega;u_1) - A(t,\omega;u_2)\|_{L_2^0} \leq C\|u_1 - u_2\|$$

and

$$\|F(t,\omega;u)\|^2 + \|A(t,\omega;u)\|_{L_2^0}^2 \leq C^2(1+\|u\|^2).$$

(vi) and the initial value ξ is $\mathcal{F}_\tau$-measurable H-valued random variable.

Definition 3.1. Suppose that $(X(t))_{\tau \leq t \leq T}$ is a random process getting values in H. $(X(t))_{\tau \leq t \leq T}$ is a mild solution of (2) if it is predictable with square integrable trajectories satisfying

$$\begin{aligned} X(t) =& S(t-\tau)\xi + \int_\tau^t S(t-r)L_1(r)X(r) + \\ &+ S(t-r)F(r,X(r))dr + \\ &+ \int_\tau^t S(t-r)A(r,X(r))dW(r) \quad \mathbb{P}-\text{a.s.} \end{aligned} \tag{3}$$

Remark 1. Since the trajectories of process $(X(t))_{\tau \leq t \leq T}$ are Bochner square integrable $\mathbb{P}$-a.s., together with Assumption 3.1, the integrals in (3) do exist.

Definition 3.2. Suppose that $(X(t))_{\tau \leq t \leq T}$ is a random process getting values in H. If $(X(t))_{\tau \leq t \leq T}$ is predictable process, its trajectories are square integrable and satisfying that $\forall v \in D(L_0^*)$ and $\forall t \in [\tau, T]$ we have

$$\begin{aligned} \langle X(t), v\rangle =& \langle \xi, v\rangle + \\ &+ \int_\tau^t \langle X(s), L_0^* v\rangle + \langle L_1(s)X(s) + F(s,X(s)), v\rangle ds + \\ &+ \int_\tau^t \langle A(s,X(s))dW(s), v\rangle \quad \mathbb{P}-\text{a.s.}; \end{aligned}$$

then $(X(t))_{\tau \leq t \leq T}$ is a weak solution of (2).

Remark 2. (i) Since $(L_0, D(L_0))$ is the generator of a C_0-semi-group $(S(t))_{t\geq 0}$ on Hilbert space H, the operator $(L_0^*, D(L_0^*))$ generates the C_0-semi-group $(S^*(t))_{t\geq 0}$. Hence, obviously that de domain $D(L_0^*)$ of L_0^* is dense in H.

(ii) For the case of linear equation with additive noise as in,[5] i.e. $F \equiv 0$ and A does not depend on time t and process X, Definition 3.2 is really coincide to[5][Def. 2.4]. Indeed, since for every $t \in [0,T]$ the operator $L_1(t)$ is bounded and $L(t) = L_0 + L_1(t)$, we have $D(L^*(t)) = D(L_0^*)$ and $L^*(t) = L_0^* + L_1^*(t)$ for all $t \in [0,T]$. Hence, for all $t \in [0,T], h \in D(L_0^*)$ we have

$$\langle X(t), L^*(t)h\rangle = \langle X(t), L_0^* h\rangle + \langle L_1(t)X(t), h\rangle.$$

For the existence of mild solution of (2), we recall the following result.

Theorem 3.1. *Under the assumption 3.1, the equation (2) has a unique mild solution. Moreover, it has a continuous modification.*

Proof. See[1][Theo. 7.4]

As a condition that weak solutions and mild solutions of (2) are equivalent, we have the following result.

Theorem 3.2. *Under the assumption 3.1, a predictable process $(X(t))_{0\leq t\leq T}$ getting values in H is a weak solution of equation (2) if and only if it is a mild solution.*

https://doi.org/10.52111/qnjs.2022.16303

Proof. Frieler and Knoche in[10] considered the time-independent non-linear stochastic differential equations with multiplicative noises. In[10][Prop. 2.10], the authors give some conditions that weak solutions to become mild solutions and vice versa. The proving Theorem 3.2 is followed by some following steps.

(i) Fix any $t \in [0,T]$ in Assumption 3.1, i.e. we reduce to the time-independent cases, the assumptions in[10][Prop. 2.10] are satisfied.

(ii) We can repeat the proving of[10][Prop. 2.10] for Theorem 3.2 if the assumptions

$$\mathbb{P}\Big(\int_0^T \|F(X(t))\|dt < \infty\Big) = 1 \quad \text{and}$$
$$\mathbb{P}\Big(\int_0^T \|A(X(t))\|^2_{L_2(U,H)}dt < \infty\Big) = 1 \tag{4}$$

are replaced by

$$\mathbb{P}\Big(\int_0^T \|F(t,X(t))\|dt < \infty\Big) = 1 \text{ and}$$
$$\mathbb{P}\Big(\int_0^T \|A(t,X(t))\|^2_{L_2(U,H)}dt < \infty\Big) = 1. \tag{5}$$

Because, in the main calculation related to F and A as in[10] we just take derivatives on the C_0-semi-group $(S(t))_{t\geq 0}$. The condition (4) just guarantees that the related integrals do exist. Hence, the condition (5) is required for the time-dependent cases.

Consider a general stochastic equation on a separable Hilbert space H as following

$$\begin{cases} dX(t) = \big(L_0X(t) + L_1(t)X(t) + \\ \quad +F(t,X(t))\big)dt + A(t,X(t))dW(t), \\ X(\tau) = \xi \in H, \quad 0 \leq \tau \leq t \leq T. \end{cases} \tag{6}$$

together with Assumption 3.1. Let $(\tilde{H}, \langle\cdot,\cdot\rangle_{\tilde{H}})$ be a Hilbert space and H be a densely and continuously embedded space in $\tilde{H}$. Denote $\|\cdot\|_{\tilde{H}}$ the Hilbert norm on $\tilde{H}$ induced by the inner product $\langle\cdot,\cdot\rangle_{\tilde{H}}$.

Assumption 3.2. Assume that $\forall t \in [\tau,T]$ the operators $S(t)$ and $L_1(t)$ are in $L\big((H,\|\cdot\|_{\tilde{H}}),\tilde{H}\big)$. Moreover, for every $t \in [0,T]$ we assume that $F(t,\cdot)$ and $A(t,\cdot)$ have extensions $\tilde{F}(t,\cdot) : \tilde{H} \longrightarrow \tilde{H}$ and $\tilde{A}(t,\cdot) : \tilde{H} \longrightarrow L_2^0(H,\tilde{H})$, respectively, satisfying Assumption 3.1, (iii)-(v) on $\tilde{H}$.

Remark 3. Let $(\tilde{L}_0, D(\tilde{L}_0))$ be the generator of semi-group $(\tilde{S}(t))_{t\geq 0}$ on $\tilde{H}$. Then due to the uniqueness of the generator of an C_0-semi-group we have $\tilde{L}_0\big|_{D(L_0)} = L_0$.

We consider the equation on $\tilde{H}$

$$\begin{cases} d\tilde{X}(t) = \big(\tilde{L}_0\tilde{X}(t) + \tilde{L}_1(t)\tilde{X}(t) + F\big(t,\tilde{X}(t)\big)\big)dt + \\ \qquad +\tilde{A}(t,\tilde{X}(t))dW(t) \\ \tilde{X}(\tau) = \xi \in \tilde{H}, \quad 0 \leq \tau \leq t \leq T. \end{cases} \tag{7}$$

Theorem 3.3. *Let Assumption 3.1 and Assumption 3.2 hold. Then each equation (6) and (7) has a unique mild solution with a continuous modification named $(X(t))_{0\leq t\leq T}$ and $(\tilde{X}(t))_{0\leq t\leq T}$, respectively, satisfying*

$$\sup_{t\in[\tau,T]} \mathbb{E}\big(\|X(t,\tau;u) - X(t,\tau;v)\|^2_H\big) \leq C_T\|u-v\|^2_H$$

and

$$\sup_{t\in[\tau,T]} \mathbb{E}\big(\|\tilde{X}(t,\tau;\tilde{u}) - \tilde{X}(t,\tau;\tilde{v})\|^2_{\tilde{H}}\big) \leq \tilde{C}_T\|\tilde{u}-\tilde{v}\|^2_{\tilde{H}},$$

for some nonnegative constants $C_T, \tilde{C}_T$ and $\forall u,v \in H$ and $\forall \tilde{u},\tilde{v} \in \tilde{H}$. Moreover, $(\tilde{X}(t,\tau;\xi))_{0\leq t\leq T}$ is an extension process of $(X(t,\tau;\xi))_{0\leq t\leq T}$ on $\tilde{H}$; i.e. $\forall\, t \in [\tau,T]$, $\xi \in H$, we have

$$\tilde{X}(t,\tau;\xi) = X(t,\tau;\xi) \quad \mathbb{P}-\text{a.s.}$$

As a consequence, we obtain the regularity of solution $(\tilde{X}(t,\tau;\xi))_{0\leq t\leq T}$ of (7) on H.

https://doi.org/10.52111/qnjs.2022.16303

Proof. Under the above assumptions, the existence and uniqueness of mild solution is obtained, see[1][Theo. 7.4]. The two inequalities follow by[1][Theo. 9.1]. We prove now the remaining task. The mild solution of equation (6) and equation (7), respectively, are

$$\begin{aligned} X(t,\tau;\xi) &= S(t-\tau)\xi + \\ &+ \int_\tau^t \big(S(t-r)L_1(r)X(r) + S(t-r)F(r,X(r))\big)dr \\ &+ \int_\tau^t S(t-r)A(r,X(r))dW(r), \end{aligned} \tag{8}$$

and

$$\begin{aligned} \tilde{X}(t,\tau;\xi) &= \tilde{S}(t-\tau)\xi + \\ &+ \int_\tau^t \big(\tilde{S}(t-r)\tilde{L}_1(r)\tilde{X}(r) + \tilde{S}(t-r)F(r,\tilde{X}(r))\big)dr \\ &+ \int_\tau^t \tilde{S}(t-r)\tilde{A}(r,\tilde{X}(r))dW(r). \end{aligned} \tag{9}$$

Let $\xi \in H$. Following the continuous extension of linear operators as in Assumption 3.2, the mild solution $(X(t,\tau;\xi))_{\tau\le t\le T}$ as in (8) also satisfies (9). Note that the uniqueness of mild solutions of (7) is up to an equivalence, among the processes satisfying

$$\mathbb{P}\Big(\int_0^T \|X(r)\|_{\tilde{H}}^2 dr < \infty\Big) = 1. \tag{10}$$

However, as in[1], if two mild solution $(X_1(t))_{\tau\le t\le T}$ and $(X_2(t))_{\tau\le t\le T}$ of (6) satisfying (10) then $\forall t \in [\tau,T]$ we have $\mathbb{P}\big(X_1(t) = X_2(t)\big) = 1$. Hence, for arbitrary $\xi \in H$ and $t \in \mathbb{R} : \tau \le t \le T$ we have

$$\tilde{X}(t,\tau;\xi) = X(t,\tau;\xi) \quad \mathbb{P}-\text{a.s.}$$

Definition 3.3. We called $(\tilde{X}(t))_{0\le t\le T}$ a continuously extended (mild) solution of (6) on $\tilde{H}$.

We consider the transition semi-groups corresponding to equations (6) and (7). Let $C_b(H)$ and $C_b(\tilde{H})$ be the space of bounded and continuous functionals on H and $\tilde{H}$, respectively. Let $\varphi \in C_b(H), \tilde{\varphi} \in C_b(\tilde{H})$ and $x \in H, \tilde{x} \in \tilde{H}$. Denote

$$P_{\tau,t}\varphi(x) := \mathbb{E}\big(\varphi(X(t,\tau;x))\big)$$

and

$$\tilde{P}_{\tau,t}\tilde{\varphi}(\tilde{x}) := \mathbb{E}\big(\tilde{\varphi}(\tilde{X}(t,\tau;\tilde{x}))\big).$$

Definition 3.4. The family $(P_{\tau,t})_{0\le\tau\le t\le T}$ is called a Feller evolution systems on $C_b(H)$ if for all $\varphi \in C_b(H)$ we have

(i) $P_{\tau,t}\varphi \in C_b(H)$ for all $0 \le \tau \le t \le T$ and

(ii) $P_{\tau,r}\big(P_{r,t}\varphi\big)(x) = P_{\tau,t}\varphi(x)$ for all $0 \le \tau \le r \le t \le T$ and for all $x \in H$.

If the two items as above satisfy for all $\varphi \in B_b(H)$, the space of bounded and measurable functionals on H, then the family $(P_{\tau,t})_{0\le\tau\le t\le T}$ is called a strong Feller evolution systems.

Theorem 3.4. *Let Assumption 3.1 and Assumption 3.2 hold. Then the families $(P_{\tau,t})_{0\le\tau\le t\le T}$ and $(\tilde{P}_{\tau,t})_{0\le\tau\le t\le T}$ are Feller evolution systems on $C_b(H)$ and $C_b(\tilde{H})$ respectively.*

Proof. The Feller property is followed Theorem 3.3 and "semi-group" property is proved by[1][Cor. 9.9].

Acknowledgements

This study is conducted within the framework of science and technology projects at institutional level of Quy Nhon University under the project code T2017.543.46.

REFERENCES

1. G. DaPrato and J. Zabczyk. *Stochastic equations in infinite dimensions*, Cambridge University Press, Cambridge, 1992.

2. R. Manthey and T. Zausinger. Stochastic evolution equations in $L_\rho^{2\nu}$, *Stochastic and Stochastic Reports*, **1999**, *66*(1–2), 37–85.

3. C. Prévôt and M. Röckner. *A concise course on stochastic partial differential equations*, Springer, Berlin, 2007.

4. M. Veraar and J. Zimmerschied. Non-autonomous stochastic Cauchy problems in Banach spaces, *Studia Mathematica*, **2008**, *185*(1), 1–34.

5. B. Baur, M. Grothaus, and T. T. Mai. Analytically weak solutions to SPDEs with unbounded time-dependent differential operators and an application, *Communications on Stochastic Analysis*, **2013**, *7*(4), 551–571.

6. M. Reed and B. Simon. *Methods of modern mathematical physics. I. Functional analysis*, Second edition, Academic Press, New York-London, 1980.

7. A. Pazy. *Semi-groups of linear operators and applications to partial differential equations*, Springer-Verlag, New York, 1983.

8. T. Kato. Linear evolution equations of "hyperbolic" type, II, *Journal of the Mathematical Society of Japan*, **1973**, *25*, 648–666.

9. D. Werner. *Funktionalanalysis*, Springer-Verlag, Berlin, 2000.

10. K. Frieler and C. Knoche. *Solutions of stochastic differential equations in infinite dimensional Hilbert spaces and their dependence on initial data*, Diploma Thesis, Bielefeld University, 2001.